OPTOGENETIC MANIPULATION OF POSTERIOR CAUDATOPUTAMEN INDIRECT PATHWAY NEURONS CAUSES AUDITORY CORTICAL ACTIVATION IN RATS

By

Zachary George Yellowman

A Thesis Submitted to the Faculty of the

COLLEGE OF MEDICINE

In Partial Fulfillment of the Requirements

For the Degree of

MASTER OF SCIENCE

WITH A MAJOR IN CLINICAL TRANSLATIONAL SCIENCES

In the Graduate College

THE UNIVERSITY OF ARIZONA

2020

THE UNIVERSITY OF ARIZONA
GRADUATE COLLEGE

As members of the Master's Committee, we certify that we have read the thesis prepared by Zachary Georgy Yellowman, titled *Optogenetic Manipulation of Posterior Caudatoputamen Indirect Pathway Neurons in Rats to Achieve Auditory Cortical Activation* and recommend that it be accepted as fulfilling the dissertation requirement for the Master's Degree.

[Committee Chair Name] Date: 01/09/2020

[Committee Member Name] Date: 01/09/2020

[Committee Member Name] Date: 01/09/2020

Final approval and acceptance of this thesis is contingent upon the candidate's submission of the final copies of the thesis to the Graduate College.

I hereby certify that I have read this thesis prepared under my direction and recommend that it be accepted as fulfilling the Master's requirement.

[Committee Chair Name] Date: 01/14/2020
Master's Thesis Committee Chair
[Academic Department]

Acknowledgments

This work would not have been made possible without the support of my family and their constant reminders of why I enjoy neuroscience research. I would like to thank Dr. Hammer and Dr. Nikulina for their guidance and mentorship throughout the process of these experiments and my time at University of Arizona. I would also like to thank Dr. Shenfeng Qiu for his help with the decision of an effective viral promotor for striatal neurons. I could not have made it through the seemingly endless days of troubleshooting wireless optogenetics without the help of both of my colleagues, Megan Rudolph and Talal Zafar.

TABLE OF CONTENTS

LIST OF TABLES

Table

LIST OF FIGURES

Figure

Abstract

Auditory hallucinations are prevalent in many neuropsychiatric disorders and are also a cardinal symptom of schizophrenia. Most research on the mechanism of auditory hallucinations has focused on functional imaging of the auditory cortex. Recent research has revealed structural and functional interaction between the striatum and the neocortex. Previous studies in our laboratory have shown that dopamine infusion into the posterior caudatoputamen (CPu), the "auditory striatum," produce activation of the rat auditory cortex. To establish the next projection site from these neurons, we virally infused an anterograde AAV-GFP into this region of the auditory striatum which resulted in expression mainly at the same rostral-caudal level of the lateral globus pallidus (LGP) as the infusion site. Since antipsychotic drugs target D_2 dopamine receptors on neurons of the indirect pathway (CPu-LGP) to alleviate psychotic symptoms, we transfected terminals in the LGP with a retrograde AAV-Jaws-GFP to neuroanatomically discriminate the indirect pathway. Inactivation of the striatal indirect pathway neurons with Jaws stimulation resulted in significant activation of the auditory cortex via c-Fos expression. Conversely, activation of these same striatal indirect pathway neurons with stimulation of ChannelRhodopsin-2 (ChR2) showed no significant change in auditory cortex activation. The results of these studies will elucidate a potential alternative neural circuit mechanism underlying the pathophysiology of auditory hallucinations in neuropsychiatric disorders.

CHAPTER 1

BACKGROUND LITERATURE

1.1 Schizophrenia and symptomology

Schizophrenia is a heterogeneous neuropsychiatric disorder that affects nearly 1% of the global population (Javitt & Sweet, 2015). The exact etiology of this disease is currently under debate; however, there exists quite a few genes and environmental risk factors that imply its underlying pathogenesis. It is often characterized by the presence of its cardinal positive symptoms- delusions and hallucinations. But sufferers from this disorder can also present with negative and cognitive symptoms. Some examples of negative symptoms include flat affect, anhedonia, social withdrawal and apathy. The cognitive symptoms present themselves as a reduction of cognitive abilities as sufferers of this disorder have been shown to have reduced IQ scores compared to the average (100 IQ) (Javitt & Sweet, 2015).

1.1.1 Prepulse inhibition as a biomarker for schizophrenia

Individuals suffering from schizophrenia have been shown to have deficits in sensorimotor gating (Mena et al., 2016). Sensorimotor gating is the ability to screen (filter) out irrelevant stimuli to grant an uninterrupted or smooth processing of more immediate sensory matters. This means that healthy individuals who have this ability are capable of habituating to repetitive stimuli or predictive stimuli. This deficit in sensorimotor gating has become a popular biomarker for those suffering from schizophrenia. Prepulse inhibition (PPI) has become a useful diagnostic test for schizophrenia as it has been shown to be present in the acute and chronic phase of the disease (Mena et al., 2016).

1.2 Pharmacological models of positive symptoms

Positive symptoms of schizophrenia can be characterized uniquely by at least three pharmacological models. The models are as follows: Overactivation of Dopamine D_2 receptor with psychostimulants, activation of serotonin 5HT2A receptors with psychedelics (LSD) and inactivation of glutamate NMDA receptors with dissociative anesthetics (i.e. phencyclidine) (Rolland et al., 2014). These models essentially depict the effectiveness of a particular

neurotransmitter/substance and its interaction with its associated receptor to induce hallucinatory or delusory symptoms.

1.2.1 Perspective of Serotonin

The ability of lysergic acid diethylamide (LSD) and other psychedelics to induce psychotic symptoms (i.e. vivid visual hallucinations) and its mechanism of action on serotonin receptors has implicated serotonin's involvement in explaining symptoms of schizophrenia. Psychedelic research has correlated the binding of 5HT2A receptors agonists and the ability to produce LSD like hallucinatory symptoms (González-Maeso & Sealfon, 2009). Transgenic mice studies have further shown the necessity of regional 5HT2A receptors in mediating a hallucinatory response. Where it was shown that cortical expression of 5HT2A receptors in mice was necessary for induction of positive symptoms (González-Maeso et al., 2007). The abnormality in 5HT2A receptors seen in patients with schizophrenia and also the effectiveness of 5HT2A antagonism with antipsychotics further establishes the importance of this receptor in explaining a mechanism of hallucinations (Vollenweider & Geyer, 2001).

1.2.2 Perspective of Glutamate

Dissociative anesthetics like phencyclidine (PCP) have been observed to induce a variety of schizophrenia-like symptoms (Rolland et al., 2014). PCP was shown to induce its psychotomimetic effects through the binding of glutamatergic NMDA receptors (Javitt & Zukin, 1991). This effect is mediated via PCP's noncompetitive inhibition of NMDA receptors. Other dissociative anesthetics such as ketamine are also shown to antagonize NMDA receptors (Javitt & Zukin, 1991). Because of these discoveries involving altered glutamatergic transmission and psychotic symptoms, researchers have been interested in the therapeutic role from stimulation of this category of receptors. Antipsychotic potential has been shown in selective agonism of metabotropic glutamate receptor (mGlu2/3) in patients suffering from schizophrenia (Patil et al, 2007). These findings alone strongly support a role of glutamate neurotransmission in the explanation the multifactorial symptomology of schizophrenia.

1.2.3 Perspective of Dopamine

The role of dopamine in psychosis became evident from studies which illustrated the ability of amphetamines, a class of drugs known to increase monoamines (i.e. Dopamine) at the synapse, to induce psychotic symptoms. However, the conclusive finding was in how effective antipsychotic medications (i.e. Haloperidol, dopamine D_2 receptor antagonist) were in treating positive symptoms of psychosis (Seeman, 2013). Additionally, studies began to correlate increase D_2 receptor presence in cases of schizophrenia where individuals suffer from hypersensitivity to drugs that increase dopamine neurotransmission (Seeman, 2013). Even though positive symptoms of schizophrenia can be explained by several pharmacological models, it is believed that they contribute uniquely to a specified phenomenological aspect of a psychotic symptom (type of hallucinatory experience) (Rolland et al., 2014). For instance, the positive symptoms resulting from agonizing 5HT2A receptors tend to be more visual than antagonism of D_2 receptors which tends to be more auditory based. The same can be said about the involvement of the glutamatergic system when explaining the phenomenology of positive symptoms. Prior studies done within our lab have shown that graded dopamine infusion within the striatum were able to induce auditory cortical activation in rats (Parga et al., 2019). These results have convinced us of a specific role that the dopaminergic system has on explaining auditory hallucinations.

1.2.4 Dopamine hypothesis

The dopamine hypothesis has been a longstanding, prominent and highly revisited theory for understanding psychotic symptoms. In Howes' and Kapur's review on the dopamine hypothesis, they emphasize the various versions of its neurochemical description and its evolution through time. With later neuroimaging studies and the effectiveness of antipsychotics, relying on high affinity for Dopamine D_2 receptors, a revised version the dopamine hypothesis was incarnated with specifications to subcortical structures and specific dopamine receptors (Howes & Kapur, 2009). The various distribution of Dopamine receptors in the brain, D_2 receptors being primarily subcortical, further emphasized the subcortical specificity of dopamine's involvement with psychotic symptoms. Lesions in the prefrontal dopamine neurons led to an increase in subcortical, striatal, dopamine levels which ultimately introduced an additional hypodopaminergic prefrontal cortex model (Pycock, Kerwin, & Carter, 1980). Prefrontal hypo-dopaminergic state was later hypothesized to be directly involved with the

negative symptoms of schizophrenia. The revised dopamine hypothesis has now begun to specify regional dopamine abnormalities with symptoms of psychosis. Unfortunately, the exact mechanisms by which dopamine was to inflict the specific symptoms of psychosis still remained undiscovered. As charming as the hypothesis made dopamine's role in psychosis to be, the etiological role in schizophrenia was elusive.

1.3 Hallucination research

A hallucination is regarded as a perceptual experience that occurs in the absence of external stimuli and must be compelling enough to be mistaken as a sensual experience (Allen et al., 2008). Taking this broader definition of auditory hallucinations into account, we subject ourselves to encapsulating a continuum of various auditory percepts that are often times only distinguished in the clinical setting or clinical research. However, considering that our level of inquiry for studying hallucinations lies on the systems/physiological level, this should be sufficient.

Although the vast majority of individuals diagnosed with schizophrenia seek clinical help due to their experience with the positive symptoms of psychosis, it is not unique to schizophrenia. Of the general population, 8% experience hallucinations and half of this population consider the overall experience distressing (Howes & Kapur, 2009). Because of the majority of individuals that have reported experiencing hallucinations, whom have not been diagnosed as having psychosis, makes the matter of understanding the mechanisms of hallucinations more urgent.

A very important phenomenological characteristic of auditory hallucinations is the perceived location. Auditory hallucinations are sometimes reported as originating from inside the head (i.e. internal auditory hallucinations) or from outside the head (i.e. external auditory hallucinations) (Blom, 2015). They can also be experienced on one side or rather both sides, giving rise to unilateral and bilateral hallucinations respectively. Even more strangely, some auditory percepts are reported from various parts of the body, such as various limbs or torso etc. These oddly located percepts have been termed extracampine hallucinations (Blom, 2015). Another critical finding pertaining to these phenomenological features of auditory hallucinations is how they tend to vary from one psychiatric disorder to another (Blom, 2015). These characteristics are very important as they themselves allude to the processing aspect of audition that has gone awry.

Traditional approaches to studying hallucinations have focused on the structural and functional neuroimaging studies. [^{18}F]Fluoro-deoxyglucose positron emission tomography (FDG-PET) has been used to observe real-time changes in cortical metabolic activity of patients with schizophrenia experiencing auditory verbal hallucinations (AVH). FDG-PET has allowed for researchers to pin-point areas such as the left frontal-temporal cortex and caudate nucleus as being hyperactive during AVHs (Horga et al., 2011). Studies utilizing arterial spin labeling, non-invasive perfusion imaging technique to monitor cerebral blood flow (CBF), have correlated increased CBF within superior temporal gyrus (auditory cortex) and dorsal striatal regions in schizophrenic patients experiencing auditory hallucinations (Zhuo et al., 2016). Functional magnetic resonance imaging with BOLD-contrast (Blood-oxygen-level-dependent imaging) is another powerful neuroimaging technique for brain activity which relies on the difference in magnetic properties of deoxygenated and oxygenated hemoglobin. Studies engaging fMRI-BOLD-contrast have been fundamental for detecting active cortical and subcortical elements during AVHs (Shergill et al., 2000). In the review paper on neuroimaging studies, patients with schizophrenia experiencing auditory verbal hallucinations tended to have decreased volumes of temporal lobe adjacent to the left insula, compared to those who are not experiencing AVHs (Bohlken, Hugdahl & Sommer, 2016). Another study found that the severity of AVHs is related to the decrease in volume of Heschl's gyrus or the primary auditory cortex (Levitan, Ward & Catts, 1999). However, other studies have reported increased grey and white matter volumes in their patients who experience hallucinations compared to non-hallucinating ones (Shin et al., 2005). Though authors of this study surmised that this result is likely due to the unmedicated state of the subjects in the study (Shin et al., 2005). To conclude, there is much speculation on the matter of explaining hallucinations in people who experience them, and the mechanism/neuro-circuitry of hallucinations remains to be discovered.

1.3.1 Rodent model of hallucinations

From the distinction in neuroanatomy alone, it is difficult to entrust rodent models with translatable data for future clinical discoveries. For example, pertaining to the basal nuclei in humans, there is a distinct separation between the caudate nucleus and the putamen by the fibrous tracts of the internal capsule. However, in rodents the caudate and putamen are not demarcated but combine into a similar but homogenous structure known as the caudatoputamen. Even though this structure appears to be homologous due to it being an undivided structure, it was found to be heterogeneous in its afferent connections with the

neocortex (Veening, Cornelissen, & Lieven, 1980). The HRP labeling study of the rodent caudatoputamen done by Veening, Cornelissen and Lieven was one of the first instances to show a topographical organization of cortical inputs at the level of the striatum and also the first to suggest a complex integratory function of several brain regions at the striatum. Even though rodent models are crucial for the discoveries in basic medical research, can we still assume that they are a reliable model for studying complex experiences such as auditory hallucinations?

In Canetta's and Kellendok's article, "Can We Use Mice to Study Schizophrenia*",* they discuss the importance of refining the animal model in characterizing the symptoms of schizophrenia and other psychiatric disorder (Canetta & Kallendonk, 2018). Positive symptoms have been notoriously difficult to model. The most commonly approached mechanism for positive symptoms of schizophrenia relates to the dopamine hypothesis and D_2 receptor hyperactivity in the striatum. This is supported by studies which have shown that enhanced occupancy of D_2 receptors by dopamine in the striatum is characteristic in drug naïve patients with schizophrenia; as well as enhanced striatal dopamine and the correlation with severity of positive symptoms (Canetta & Kallendonk, 2018).

However, schizophrenia's positive symptoms effect individuals specifically and are often times characteristic of the patient. This is why it is crucial to emphasize specific circuity-based approach to delineate the experience of positive symptoms. The overexpression of D_2 receptors in the striatum of mice have shown to impair spatial working memory and associative learning, these of which are tasks traditionally associated with medial prefrontal cortex function (Canetta & Kallendonk, 2018). An example from our research is elucidating the function of the posterior striatum in rodents regarding auditory cortex activation. This finding is important as it suggests a potential pathway that might be involved with internally generated auditory experiences or perceptions of sound. Which we believe is crucial towards developing more sophisticated animal models of auditory hallucinations, as well as furthering our understanding of hallucinations in general.

1.4 Basal ganglia and posterior striatum

The basal ganglia are a group of subcortical nuclei that are largely responsible for motor and sensory decisions, or also neatly summarized as psychomotor behavior and procedural/associative learning (Ring, 2002). The striatum is a region of the basal ganglia that receives the majority of cortical inputs (Ring, 2002). This region has generally been demarcated

into ventral striatum, which contains the nucleus accumbens and the olfactory tubercle, and the dorsal striatum which includes the caudate nucleus and putamen. However, recent findings suggest that a functional segregation of the striatum is important for understanding the function of this structure (Hunnicutt., Jongbloets. et. all, 2016). When a functional demarcation of the striatum is considered, we now have the four domains, sensorimotor, limbic, associative and a fourth posterior domain. The posterior striatum has been shown to be involved with auditory and visual processing. However, the precise demarcations of these functional subdivisions are relatively new and only recently have studies tried to thoroughly study these boundaries (Hunnicutt., Jongbloets. et. all, 2016). This approach to elucidating the striatum is important as the consideration of the striatum for auditory hallucinations has largely gone unnoticed (Figure 1).

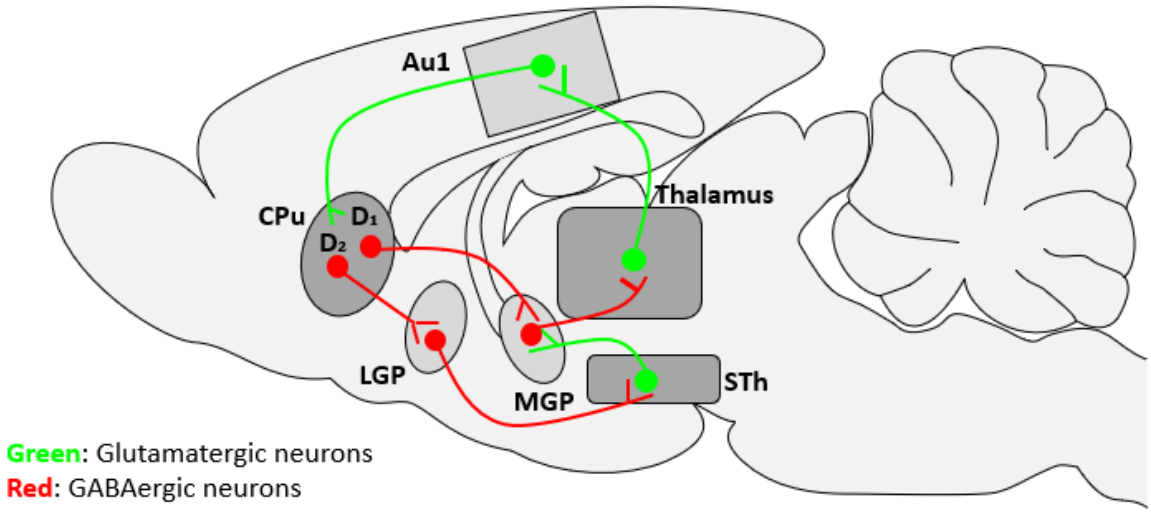

Figure 1. Simplified illustration of Cortico-Striatal-Pallidal-Thalamo-Cortical loops in sagittal illustration of rat brain. Inspired by Parkinson's disease motor studies and sensory studies showing auditory cortex projections in striatum (Wichmann & Dostrovsky, 2011) (Chen et al., 2019).

A region of the posterior striatum- tail of the caudate, is known to participate in visual processing (Seger, 2013). Seger discusses in this review the difficulty of studying this neuroanatomical structure due to a lack of sensitivity in measuring the activity of this region with neuroimaging techniques and a poor non-human animal model. To emphasize his point, the tail of the caudate

nucleus is often times overlooked. Even though this structure has recently been shown to have an important role for both visual and auditory processes.

A recent study by Liang Chen and Xingxing Wang looked into the aspects of this posterior region of the striatum for auditory processing and have found afferent connections from both auditory cortex and auditory sensory thalamus (medial geniculate body of thalamus) (Chen et al., 2019). They used chemogenetics to silence these connections to show their involvement with auditory frequency discrimination in mice. They concluded that the MGB medium spiny neurons functions mainly as a gain controller- discriminating frequencies at a broad range and the auditory cortex medium spiny neurons provide tuning information of sounds (Chen et al., 2019). This is a crucial finding as it further clarifies the role of auditory processing in the fourth functional subdivision of the striatum- tail of the striatum. Additionally, much earlier studies of auditory cortices involvement in the basal ganglia, have shown that picrotoxin (noncompetitive GABA-A receptor antagonist) infusions into the auditory cortex results in ipsilateral expression of c-*fos* in the caudal striatum (Arnauld et al, 1996). These results validate a theory of a posterior region of the striatum that is involved with auditory processing. However, to the best of our knowledge no such studies have been able to establish the full cortico-striato-pallido-thalamo-cortical loop at the topographical level of the auditory cortex (Figure 1).

The posterior striatum has a stable representation of sounds which implies an importance for auditory decisions (Guo, Walker, et al., 2018). Their results showed that activation of the posterior striatum had no effect on motor initiation; instead it was shown that this region is involved with auditory decisions. They were able to show through bilateral injections of muscimol (GABA-A Receptor agonist) into the posterior striatum resulted in an impairment of auditory decisions as compared to saline control (Guo et al., 2018). These results support the need for our study to confirm the striatal-pallidal-cortical within in the posterior striatum.

1.5 Optogenetics and neuronal excitation

Optogenetics provides a temporally and spatially effective way of activating or inactivating neurons. Optogenetics grants the ability to be able to specifically turn on or off neurons that have been transfected with optically active ion channels. This technique has allowed researchers to correlate circuit level neuron activity *in vivo* to study animal behavior (Britt, McDevitt, and Bonci, 2012). In our experiment we will be utilizing Channelrhodopsin-2 and Jaws to manipulate neurons posterior striatum within the indirect pathway.

Channelrhodopsin-2 (ChR2) is found within the algae *Chlamydomonas reinhardtii*. These 7 transmembrane domain protein channels provided algae with the perception of light (Lin, 2011). ChR2 is a non-selective cation channel which is capable of depolarizing neurons once activated by light (Britt, McDevitt, and Bonci, 2012). The appropriate wavelength of light for achieving a sufficient response from ChR2 is 473nm blue light. In previous studies done in our lab, we have found that 10hz stimulation with 473nm light was sufficient enough to elicit a c-Fos response in cells directly affected by channelrhodopsin-2.

Stimulation of ChR2 at 10Hz was shown to be effective in activating neuronal activity in a variety of studies. Striatal glutamatergic activation, in transgenic mice expressing ChR2, with 473 nm blue light at 10Hz resulted in Ca^{2+} influx and increased membrane currents (Song et al., 2017)**.** In the same study, it was shown that laser power ranging from 0.35 to 1.02 mW was sufficient to achieve the desired neuronal activity. Another study focused on the use of ChR2 transgenic mice in exploring olfactory processing, was able to show that neuronal spike generation is very reliable for stimulation frequencies ranging from 10 to 40 Hz (Arenkiel et al., 2007). The frequency parameter of 10Hz is therefore a highly reliable way of activating neurons with the ChR2 actuator.

Silencing neurons with the use of optogenetically active chloride ion and proton pumps has also been a powerful technique for causally assessing neuronal circuit function. However, the ability to silence larger quantities of tissue became difficult due to the penetrability of light used to activate these opsins. The Red-shifted Cruxhalorhodopsin, Jaws, was discovered from the shark strain of *Haloarcula salinarum*. After some additional modifications were made to improve light induced photocurrents and its expression in neurons; It was found to be a powerful addition to the toolset of inhibitor type opsins (Chuong et al., 2014). Compared to previous optogenetic inhibitors, Jaws was found to produce higher light induced currents upon red light stimulation. Jaws is capable of mediating these inhibitory photoinduced currents through changes in chloride ion conductance (Chuong et al., 2014). The penetrability of 632 nm red light allows Jaws to be activated in sparser/deeper regions of the brain and has even been shown to be activated from a transcranial red-light source. This is likely due to longer wavelengths of light having less interaction with blood proteins and lipids (Chuong et al., 2014).

Inhibitor opsins work best at the lower frequency stimulation parameters. This is due to the effect of having a post-illumination rebound. Jaws was shown to be activated with 1s pulses at 0.1 Hz with various light intensities (10, 25, 50, 75 mW/mm^2) (Chuong et al., 2014). The parameters we decided to test with our pulsatile receiver are 8s pulse at 0.1 Hz and 3s pulse at

0.3 Hz. Due to the prevention of overheating the battery on our pulsatile receiver, we deemed these near continuous parameters as sufficient for testing.

There are several ways of incorporating optogenetic genes within the desired animal. Some of these are electroporation, transgenic animals or by transfection with virus. The viral method for delivery of optogenetic genes is very common due to its rapidity and relatively simple method of viral delivery. It is crucial to restrict expression of the opsin to certain neurons to achieve experimental specificity (Britt, Mcdevitt, and Bonci, 2012). Researchers can utilize a cre/lox system to mediate viral expression of optogenetic genes. This is done by utilizing transgenic cre-expressing mice to limit the ability of viruses to express opsin genes only in the presence of cre recombinase. The cre recombinase is able to perform recombination at specific sites in the viral DNA allowing for opsin expression (Britt, Mcdevitt, and Bonci, 2012). This results in only neurons with sufficient levels of cre recombinase to have opsin expression.

1.5.1 Wireless optogenetics

Wireless optogenetics offers an unimpeded optogenetic approach while actively observing animal behavior. Utilizing the Amuza's Teleopto wireless optogenetic system for our studies, we will be implementing light emitting diodes (LED) source with implantable fiber optics. There are two choices of a light source for optogenetics that include diode-pumped solid-state lasers (DPSS) and light emitting diodes (LEDS). Lasers and LEDs are both characterized by their wavelength and light intensity. However, LEDs have the advantage of being less expensive. LEDs are also supplied in a wide variety of wavelengths and are smaller which allows for a more mobile approach to tissue stimulation. However, when compared to lasers LEDs can suffer on the intensity of light delivered. This was seen as a problem as sufficient light intensity is required to provide activation while also concerned with minimization of tissue heat (Britt, Mcdevitt, and Bonci, 2012). However, these issues were considered in preliminary studies done in our lab with LED wireless optogenetics. We have not had any observable issues with tissue heat while running our stimulation parameters at the predicted light outputs (5-10mW range).

1.5.2 c-Fos as an indirect marker of neuronal activity

Since it was identified as a proto-oncogene (Curran et al, 1984), the immediate early gene (IEG) *c-Fos* and its associated Fos protein has long been used as an indirect marker of

neuronal activity. The family of Fos proteins, which include c-Fos, FosB, Fos-related antigen 1 and Fos-related antigen 2, are categorized as nuclear oncogenes. The expression of Fos protein is relatively rapid and is induced by a variety of extracellular factors (Chung, 2015). Once translated, the Fos protein will dimerize with an associated Jun protein to form Activator Protein-1 which acts a transcription factor. In the event of neuronal depolarization, intracellular calcium signaling occurs mainly from L-type voltage-sensitive calcium (VSCC) and glutamate receptors (NMDAR) (Chung, 2015). These signaling events have been shown to induce *c-Fos* m-RNA and Fos protein expression. Because of the instability of *c-Fos* mRNA and auto-repression of the mRNA from the Fos protein, there are very low constitutive levels of c-Fos. This low level of basal c-Fos expression makes it an ideal marker for neuronal activation.

There are also some aspects of c-Fos expression that reduce its effectiveness as a marker for neuronal activity. The levels of c-Fos expression can vary substantially with repetitive stimulation (Chung, 2015). This is due to neural plastic changes that occur which can either sensitize or desensitize depending on the change. Although this phenomenon does make *c-Fos* a unique way to measure physiological changes that occur during learning.

1.6 Research question

The importance of functional subdivisions within the auditory striatum have recently begin to emerge with studies aiming towards a delineation of function regarding auditory cortical and sensory thalamic afferents terminating within this region (Chen et al., 2019). To the best of our knowledge, a complete cortico-striatal-pallidal-thalamo-cortical loop as suggested in Figure 1, remains to be fully established for the auditory cortex. The discovery of such a model we believe has profound implications in the fields of psychiatry and others interested in modeling auditory hallucinations. We know from previous studies that hyperdopaminergic activity in the striatum is correlated with positive symptoms of schizophrenia and also presents a well-established, common model for representing these states of mind (Canetta & Kallendonk, 2018). We hypothesize that inactivation of striatal-pallidal neurons within the indirect pathway of the posterior striatum (caudatoputamen in rats) with stimulation of Jaws will produce an effect similar to enhanced dopamine D_2 receptor activity and result in auditory cortex activation. We also hypothesize that activation of striatal-pallidal neurons within the same indirect pathway of the posterior striatum with ChannelRhodopsin-2 will produce an effect similar to impoverished dopamine D_2 receptor activity and result in less auditory cortex activation.

CHAPTER 2

DEFINING THE POSTERIOR STRIATAL/PALLIDAL PATHWAY IN RODENTS AND OPTIMIZATION OF OPTOGENETIC PARAMETERS FOR THE USE OF JAWS AND CHANNELRHODOPSIN-2

2.1 Project Summary

Background: The precise projection locations of the posterior striatal neurons in the rodent caudatoputamen to the lateral globus pallidus have not been fully ascertained in our lab. The stereotactic location of these striatal terminal projections in the lateral globus pallidus is crucial for our future experiments involving opsin expression in the posterior striatum. Utilizing the same coordinates previously used in our lab to achieve zif268 mRNA expression in the auditory cortex of rodents via graded dopamine infusions, we will label this connection from the posterior striatum to the pallidum via an anterograde adeno-associated virus expressing GFP (Parga et al., 2019). The terminals will be confirmed with fluorescent microscopy.

The optogenetic parameters for stimulating and inhibiting the striatal-pallidal indirect pathway neurons needed to be confirmed for this region. Previous studies support a continuous set of stimulation parameters for activating Jaws (Chuong et al., 2014). However, our lab does not acquire the devices to simulate these continuous conditions for Jaws activation. However, we intend on utilize a pseudo-continuous set of parameters in this preliminary experiment to determine which one is more effective at activating the Primary (M1) and Secondary (M2) motor cortices. The parameters for stimulating the indirect pathway with channelrhodopsin were determined by previous experiments in our lab via successful stimulation of infralimbic cortex to ventral tegmental area projection neurons.

Methods: The locations of the anterograde projections of AAV-hSyn-GFP (50465-AAV5, addgene) two weeks after unilateral infusion in the posterior caudatoputamen in rodents were analyzed. Retro viral expression of AAV-hSyn-Jaws-KGC-GFP-ER2 (#65014-AAVrg, addgene) requires 6 weeks for optimal expression. After the optimal expression period of the retrograde AAV-Jaws in rodents involved in the parameter study, they were surgically implanted with a unilateral fiber optic (630nm, 0.67 NA, 0.5mm Diameter, Teleopto). After a three-day postop the rats involved in the parameter study were habituated for several days until stimulation. The brains were then serially sectioned to span a millimeter of lateral globus pallidus tissue near respective infusion sites. The tissue was then imaged using the M2 Epifluorescent Axioskop microscope to assess GFP expression.

Optogenetic parameters: The set of parameters used for pseudo-continuous stimulations: 8 second pulse at 0.1 Hz (Parameter A) with 630nm light for a 30-minute period; and 3 second pulse at 0.3 Hz (Parameter B) with 630nm light for a 30-minute period.

Behavioral paradigm: On stimulation day rats were given a 20-minute habituation period after the wireless receiver was fitted, followed by the 30-minutes of optogenetic stimulation with the respective parameters, and then were perfused an hour following the stimulation to allow adequate c-Fos expression.

Results: The images showed distinct expression in the lateral globus pallidus (LGP) following correct infusion of AAV-hSyn-GFP in the posterior caudatoputamen (-1.8mm A/P, +4.3mm M/L, -6.0mm D/V). The expression was lateral in the LGP, closest to the caudatoputamen. The approximated coordinates of maximum expression were ascertained to be around -1.8mm A/P, +3.9mm M/L and -6.0mm D/V.

There was no observed difference in locomotion from the two pseudo-continuous optogenetic stimulation parameters. There was also no significant difference in c-Fos expression in motor cortices resulting from the different optogenetic parameters.

Conclusion: The results of this tracing study have allowed for us to determine the stereotactic location of our target in the LGP for the infusion of retro-AAV-JAWS/ChR2-GFP. We have decided to utilize the 3s-ON and 100ms-OFF (Parameter B) pseudo-continuous parameters for Jaws. This parameter has less light-off time and appears to run well with the equipment. The parameters 10Hz 1-minute stimulation will be used for ChannelRhodopsin-2. These parameters have shown to be sufficient for studies requiring neuronal activation with the respective opsins.

2.2 Experimental Design/Animals

Subjects: The viral tracing study consisted of 12 Sprague Dawley rats received from Charles river laboratory. The operating weight was maintained at 250 grams, this would ensure the most accuracy when referencing the stereotactic coordinates from the Paxinos and Watson atlas. The optogenetics studies included 2 for pseudo-continuous parameter optimization and 1 for the optimization of channelrhodopsin. These were Long Evans rats around 250 grams. All Animals were group-housed in a controlled environment with 12-hour reverse light/dark cycle housing. Food and water were available *ad libitum*. These experiments were all approved by the University of Arizona Institute of Animal Care and Use Committee.

2.3 Intracerebral viral infusion and Fiber Optic Implantation

During stereotaxic surgery, 2-4% continuous supply of isoflurane gas was administered using a vaporizer and fume evacuator. Each subject was administered a 1mg/kg dose of meloxicam (Alloxate) for post-surgical analgesia. Unilateral craniotomies were performed and 1 μl of AAV2-hSyn-eGFP (#50465-AAV2, addgene) at a titer of $3x10^{12}$vg/mL was unilaterally infused into the posterior caudatoputamen (-1.8 A/P, +4.5 M/L, -6.0 D/V, 0˚ tilt, from Paxinos and Watson, 2007). Approximately 2 weeks later, brains were collected for striatal projection analysis. Brains infused with 1 μl of AAV-hSyn-Jaws-KGC-GFP-ER2 (#65014-AAVrg, addgene) at a viral titer of $1.3x10^{13}$ GC/mL at coordinates (-0.8mm A/P, +2.9mm M/L, -6.0mm D/V, 0^0) were implanted with unilateral LED fiber optrodes (0.5mm diameter, 0.67 NA, 630nm, 10mW output, Teleopto, Nagoya, Japan) into the identified region of the rostral striatum. Output of LED fiber was deemed effective for Jaws stimulation by use of the "Predicted irradiance calculator" (Figure 2) from the optogenetics resources at Stanford University. This calculator was formulated from measurements of light penetrance in mammalian tissue and was used to determine our fiber optic output (10mW) for achieving an irradiance of roughly 0.1mW/mm^2 at tissue depth of 2 mm.

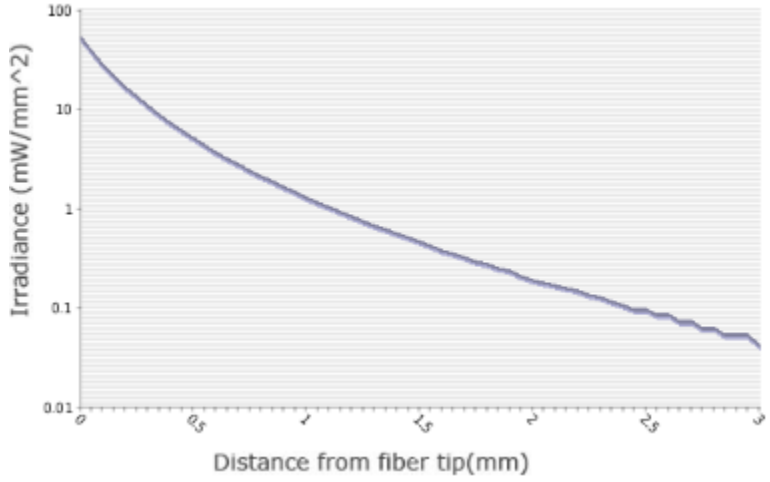

Figure 2: Predicted irradiance (mW/mm^2) given numerical aperture of fiber (NA 0.67), power output (10 mW) and diameter of fiber (0.5mm) ("Predicted irradiance calculator", Optogenetic Resources at Stanford University, 2019).

2.4 Data and Tissue analysis

2.4.1 Euthanasia and brain extraction

Animals were euthanized after receiving intraperitoneal injection with Euthasol sodium pentobarbital (200 mg/kg, i.p.) and transcardial perfusion with % paraformaldehyde (0.9% NaCl) for tissue fixation followed by decapitation by guillotine. These euthanasia methods are consistent with recommendations of the American Veterinary Medical Association Panel on Euthanasia.

Once animals have received their i.p. injection with Euthasol they were anesthetized with isoflurane and were then transcardially infused with 15 mL of 1X PBS solution with Heparin. Following this infusion, animals were transcardially infused with approximately 250 mL of 4% Paraformaldehyde (0.9% NaCl). Animals brains were extracted and placed in a 4% Paraformaldehyde (0.9%) solution for 90 minutes. Following this period, brains were then placed in graded sucrose solutions (12.5% sucrose overnight, 25.0% sucrose until freezing). Freezing tissue involved coating the animal brain in O.C.T. (Optimal Cutting Tissue medium) and then snap freezing in crushed/powdered dry ice for roughly 60 seconds. These brains were then stored in a -80^{0}C freezer until sectioning

2.4.2 Immunohistochemical analysis and imaging

The CM195 Leica Cryostat was used to section frozen brain tissue which was then collected onto microscope slides. These slides were vacuum dried for 10 minutes and stored overnight in a 4^{0}C freezer prior to being stored in 80°C freezer until immunohistochemical procedures. The tissue infected with AAV2-hSyn-GFP (#50465-AAV2, addgene) were washed with 0.05M KPBS (pH=7.4) for 5 minutes prior to being coverslipped with ProLong™ Diamond Antifade Mountant (Invitrogen, P36970) to protect the slides for prolonged imaging. These slides were then imaged on the M2 Epifluorescent Axioskop microscope to visualize the expression in the lateral globus pallidus.

The optogenetically stimulated animals were blocked with 5% Normal goat serum (0.05M KPBS, 0.4% Triton-X) for 1-hour prior to being stained with Phospho-c-Fos (Ser32) (D82C12) XP® Rabbit mAb (#5348, Cell signaling) antibody at 1:200 dilution for 48-hour period. The slides were then incubated with the Alexa Fluor-594 goat anti-rabbit IgG secondary antibody (Invitrogen, R37117) for a 45-minute period. Three 5-minutes washes in 0.05M KPBS (pH=7.4) were done in between antibody incubations.

2.4.3 Statistical analysis

Motor cortices were analyzed at approximately (-0.8mm A/P). Three 20μm sections that resembled the aforementioned region were chosen for each animal and analyzed via automated cell counts with ImageJ Fiji software to produce a mean labeling profile of the given region. Parameters for the automated cell counts are 0.5-1.0 circularity, 30-255 image threshold and 100-10000 pixel cell area. The total area used to count c-Fos expression was about 4.0mm^2. Immunohistochemical data were analyzed via nonparametric statistical tests with unpaired t-test with Welch's correction utilizing Prism statistical software. We determined statistical significance to be satisfied if the resulting p values ≤ 0.05.

2.5 Immunohistochemistry and Fluorescent imaging results

2.5.1 Tracer study results

Viral infusion into the posterior striatum (-1.8mm from bregma) resulted in lateral expression of green fluorescent terminals in the lateral globus pallidus (Figure 3). The most intensive labeling of GFP terminals were observed in the lateral globus pallidus at the same rostral-caudal level as the infusion site. Shown in Figure 4, terminal expression was also observed in the reticular thalamus (Rt), medial globus pallidus (MGP) and subthalamic nucleus (STh). However, we are only interested in the LGP projections, as these connections form the bulk of the indirect pathway. The location of these terminals can be approximated with the following stereotactic coordinates (-1.8mm A/P, +3.9mm M/L, -6.2mm D/V, 0^0). This location will be the target of our retrograde adeno-associated virus expressing its associated opsin (ChR2 or Jaws).

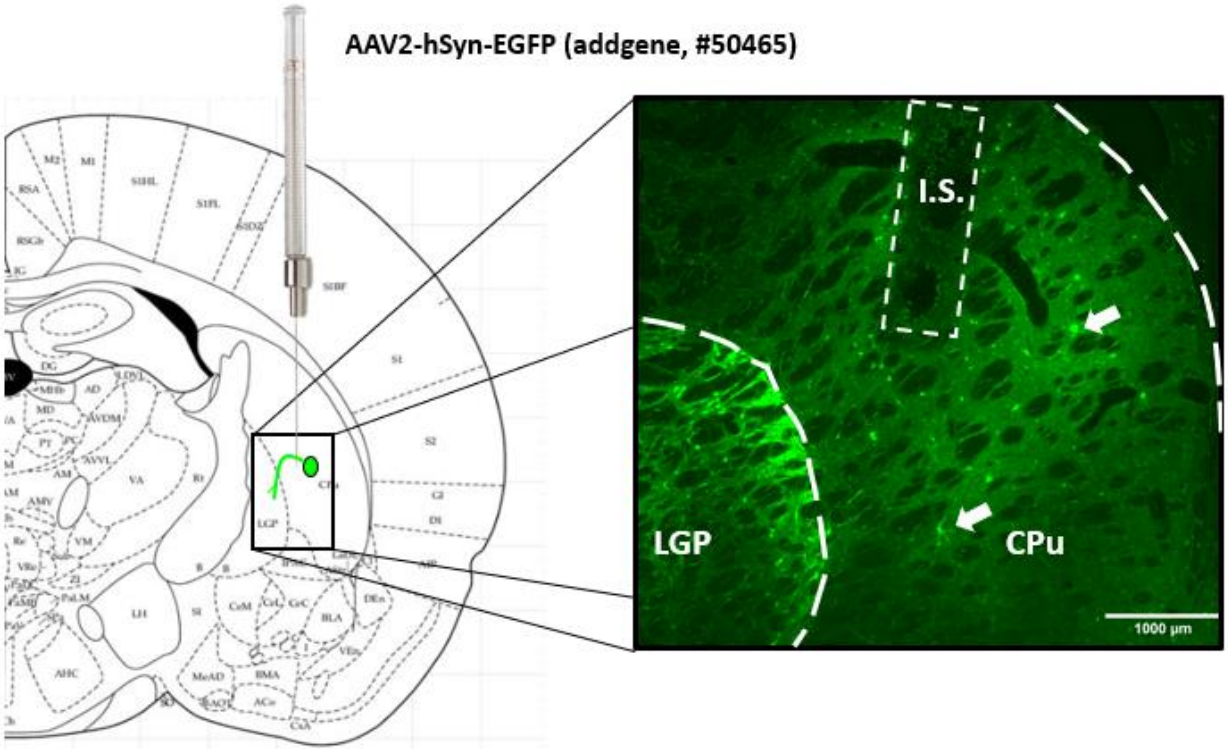

Figure 3. Viral infusion of AAV2-hSyn-eGFP (#50465, addgene) into CPu (-1.8 A/P, +4.5 M/L, -6.0 D/V, 0˚ tilt, from Paxinos and Watson, 2007). Neurons in CPu are marked with white arrows, dashed white line demarcates LGP from CPu. Scale bar at 1000 µm.

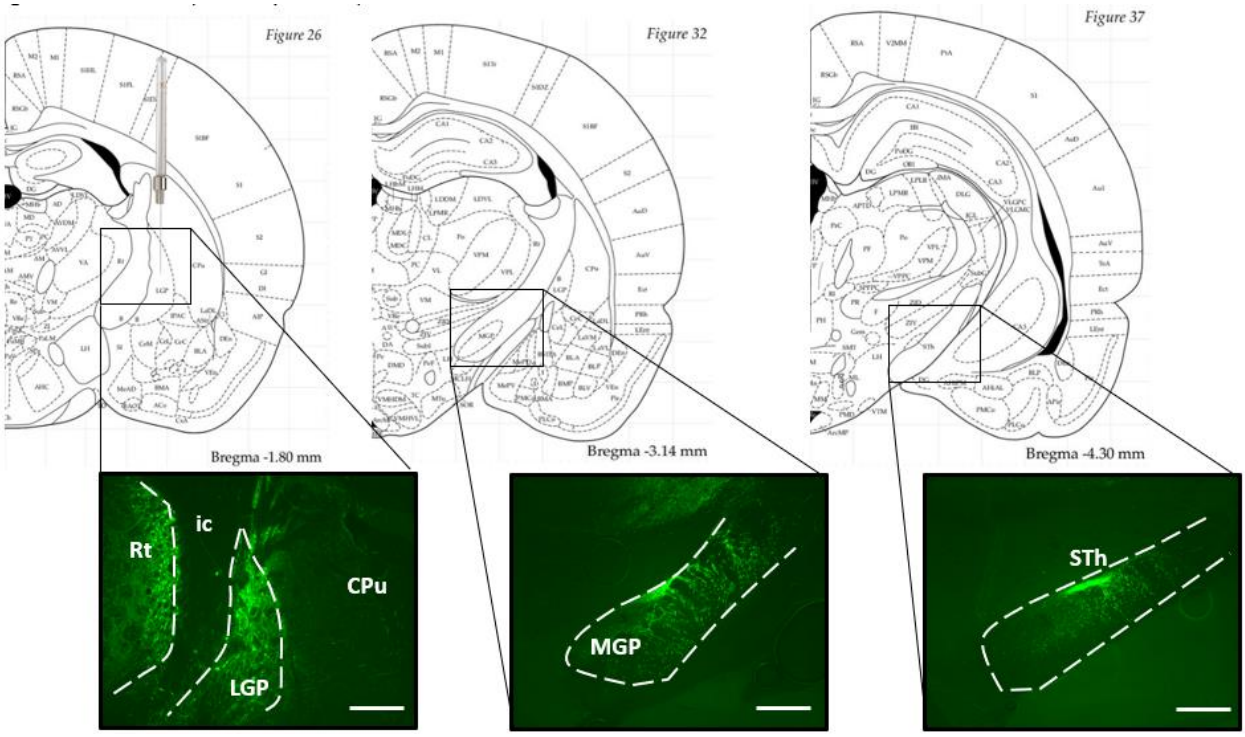

Figure 4. Viral infusion of AAV2-hSyn-eGFP (#50465, addgene) into CPu (-1.8 A/P, +4.5 M/L, -6.0 D/V, 0˚ tilt, from Paxinos and Watson, 2007). Expression seen also in reticular thalamus (Rt), medial globus pallidus (MGP) and subthalamic nucleus (STh). 1000 μm scale bar.

2.5.2 Motor study Infusion site

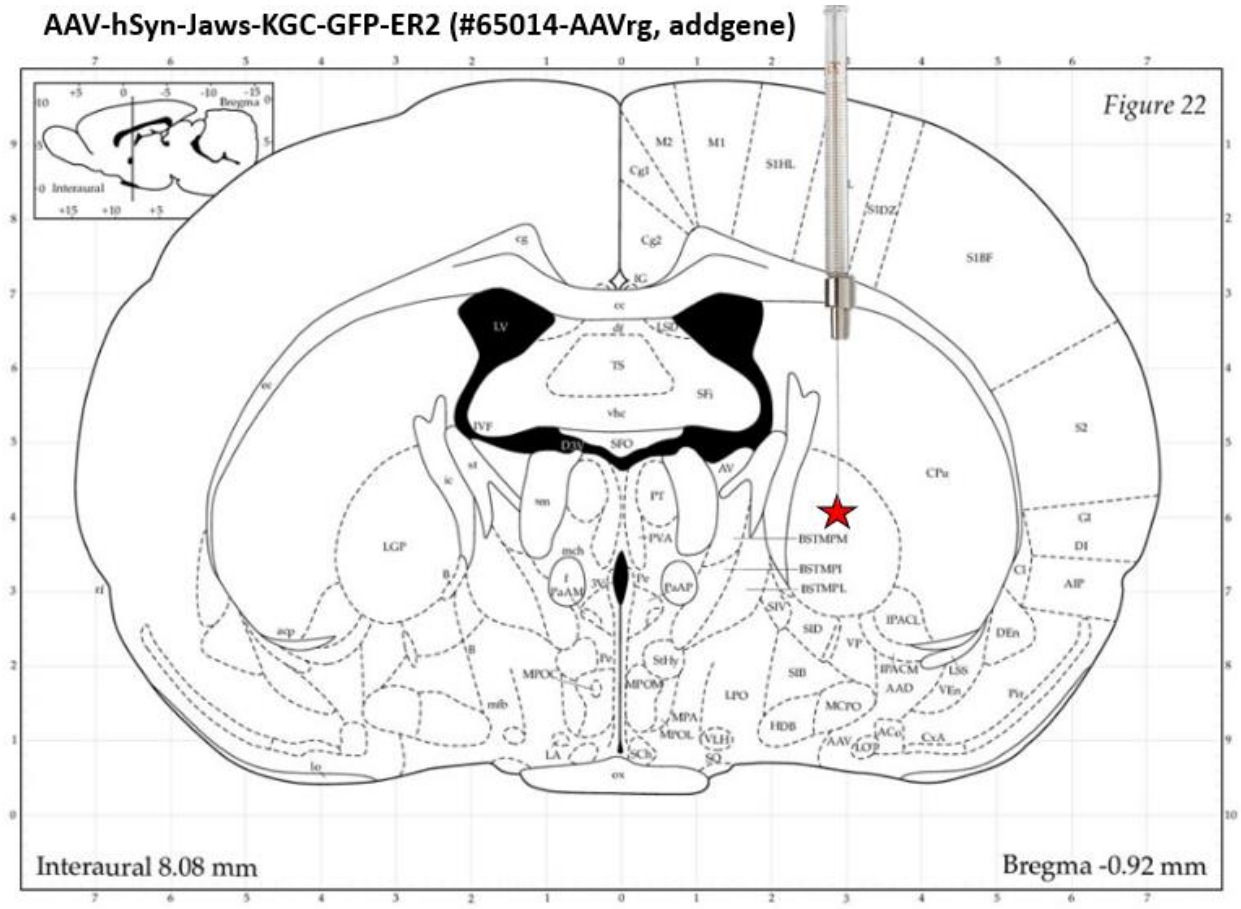

Figure 5. Red star indicates infusion site of retrograde AAV-hSyn-Jaws-KGC-GFP-ER2 (#65014-AAVrg, addgene). Infusion coordinates (-0.8mm A/P, +2.9mm M/L, -6.0mm D/V, 0^0) Gaidica, M. (2019). Rat Brain Atlas. Retrieved 16 December 2019, from http://labs.gaidi.ca/rat-brain-atlas/.

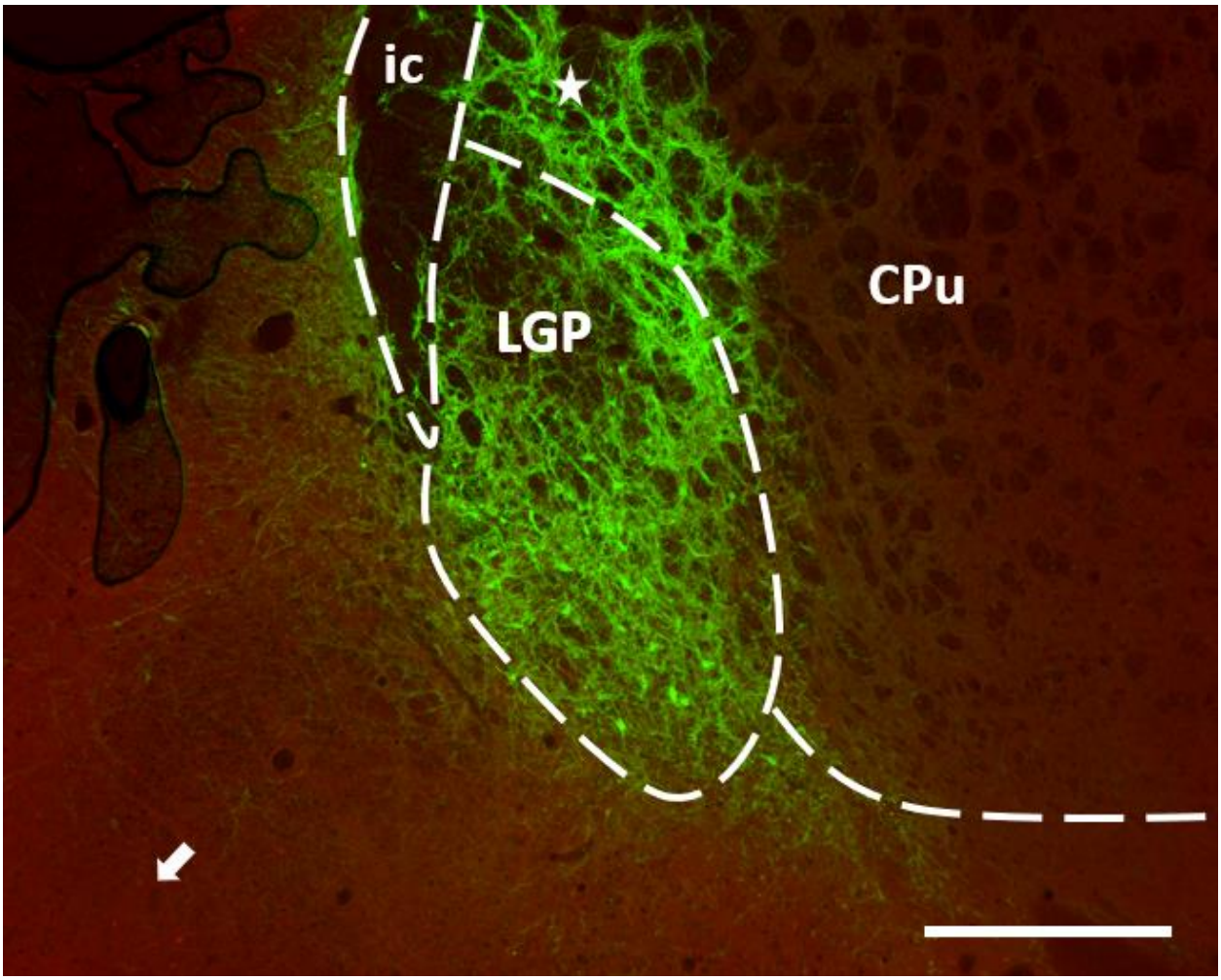

Figure 6. Expression of GFP from viral infusion of retrograde AAV-hSyn-Jaws-KGC-GFP-ER2 at stereotactic coordinates (-0.8mm A/P, +2.9mm M/L, -6.0mm D/V, 0^0). Arrow indicates c-Fos expression. Star indicates striatal neuron expressing GFP in CPu. Scale bar 1000μm.

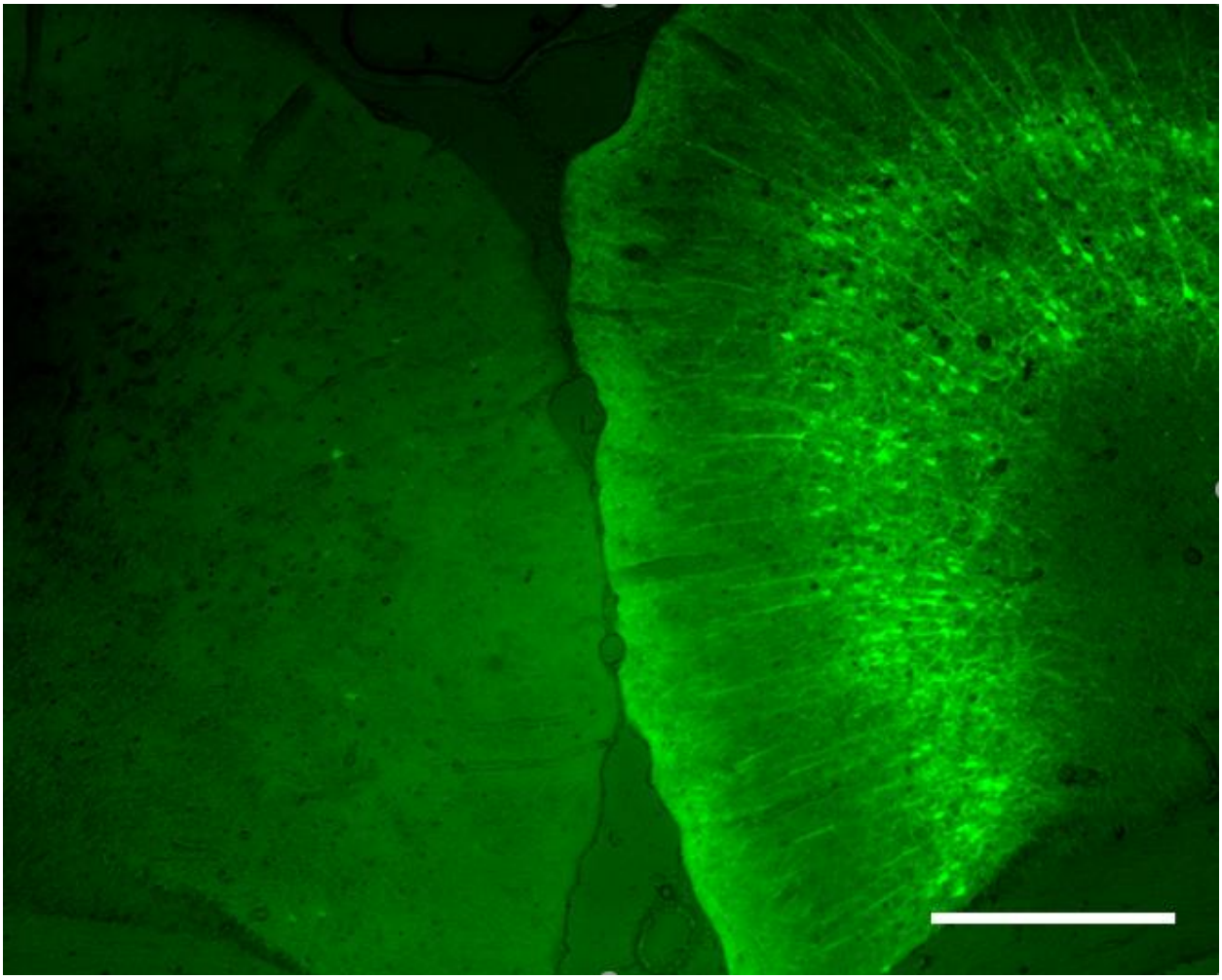

Figure 7. Green Fluorescent Protein expression in motor cortices from infusion of retrograde AAV-hSyn-Jaws-KGC-GFP-ER2 at stereotactic coordinates (-1.0mm A/P, +2.9mm M/L, -6.0mm D/V, 0^0). Scale bar 1000μm.

Infusion of the retrograde AAV-hSyn-Jaws-KGC-GFP-ER2 into a rostral potion of the striatum (Figure 5) known to be more influenced with motor activities resulted in expression lateral CPu (Figure 6) and ipsilateral cortical expression (Figure 7). Cortical expression shown in Figure 7 illustrates the primary motor cortex connections with the LGP at this rostral/caudal level (-0.8 A/P). There was little to no expression of c-Fos in the LGP and adjacent CPu. However, c-Fos can be detected in the medial thalamic regions shown in Figure 6.

2.5.3 Difference in c-Fos expression between optogenetic parameters

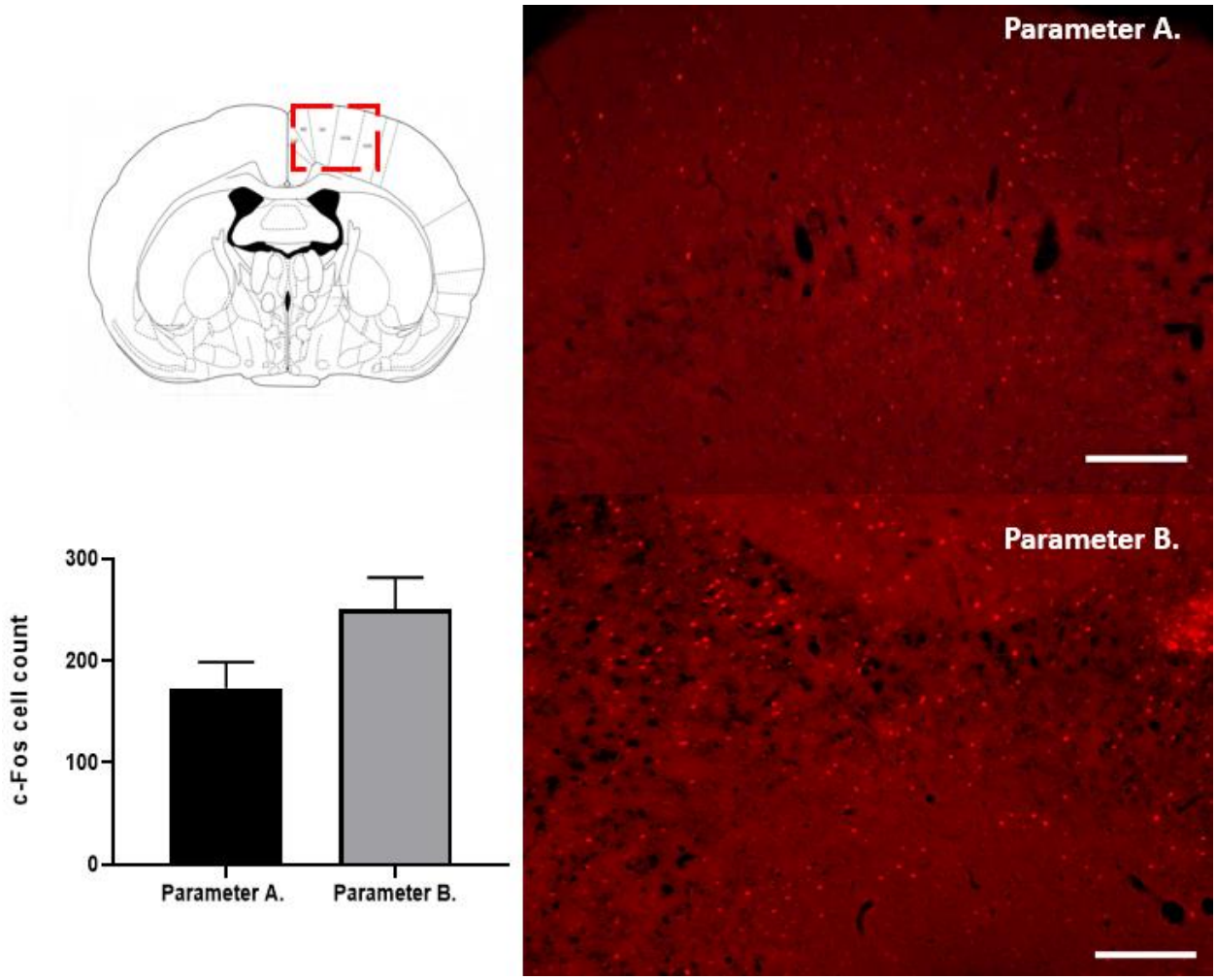

Figure 8. Expression of c-Fos in primary (M1) and secondary (M2) motor cortices of rat. Red box illustrates the approximate region of stereotactic image where images on the right were taken. Parameter A) denotes the c-Fos expression resulting from 8s light pulse at 0.1Hz. Parameter B) denotes the c-Fos expression resulting from 3s light pulse at 0.3Hz. Scale bar 500μm. Graph depicts c-Fos cell counts.

	Virus	Stimulation	Cell count (c-Fos) s1	s2	s3	Mean cell count	Unpaired t-test Welch's correction	F test comparison of variances
Motor R2	Jaws	8s pulse 0.1 Hz (parameter A)	199	122	198	173	P-value =0.1314	P-value=0.7955
Motor R3	Jaws	3s pulse 0.3 Hz (Parameter B)	313	216	222	250.33333	Result = ns	Result = ns

Table 1. Illustrates the c-Fos cell counts for both parameters and the statistical analysis summaries. Area of analysis is roughly 4 mm^2.

The expression of c-Fos in motor cortices was more prominent after stimulation of Jaws with parameter B (3s pulse at 0.3Hz). However, the amount of c-Fos expressed from comparison of both parameters showed no significant differences (Table 1).

2.6 Discussion

The results of the tracing study have specified the stereotactic coordinates that will be utilized in a future study involving the expression of optically sensitive ion channels (opsins) in the indirect pathway of the posterior caudatoputamen. This experiment was necessary as we were uncertain of the specific rostral-caudal region of the lateral globus pallidus (LGP) which was being projected to from the posterior region of the caudatoputamen (auditory striatum). The region with the most terminal expression was found to be in the same rostral-caudal axis as the infusion site into the posterior caudatoputamen. We determined the coordinates for our retrograde adeno-associated virus in experiment 2 to be (-1.8 A/P, +3.9 M/L, -6.0 D/V, 0° tilt, from Paxinos and Watson, 2007) in the LGP.

We know from studies by Boyden's lab that continuous parameters for stimulation of Jaws are optimal (Chuong et al., 2014). However, we do not possess a wireless receiver capable of running continuous parameters without damaging the equipment. Instead, we decided to test two pseudo-continuous parameters, in the motor striatum, to ascertain which would be better at activating the motor cortex. Inactivation of the indirect pathway in the motor striatum (-0.8mm A/P, +2.9mm M/L, -6.0mm D/V, 0^0), was theorized to activate the motor cortex and possibly produce contralateral movement in the rats. The results of the optimization of optogenetic parameters showed no significant difference in c-Fos expression between Parameter A (8s pulse, 0.1Hz) and Parameter B (3s pulse, 0.3Hz). The mean number of cells expressing c-Fos (250 cells/4mm^2.) was larger in parameter B. We have decided to utilize Parameter B due to it appearing to have more of a c-Fos

response. We believe this is likely due to Parameter B resembling a more continuous light source, when compared to Parameter A. Therefore, we will be using the 3s pulses at 0.3Hz parameter in our next experiment for stimulating Jaws in striatal neurons of the indirect pathway.

CHAPTER 3

OPTOGENETIC MANIPULATION OF THE INDIRECT STRIATAL PATHWAY TO AUDITORY CORTEX

3.1 Project summary

Background: The auditory striatum has recently begun to emerge as a prominent striatal pathway for regulating elements of auditory information. Earlier studies done within our lab have shown that a posterior region in the caudatoputamen of rats, when infused with dopamine, is capable of activating the primary auditory cortex. This region of the caudatoputamen can be described as being analogous to an auditory striatal region. However, the precise locations of these auditory striatal projections have just recently been established through viral tracing studies done within our lab to terminate mainly in the adjacent lateral globus pallidus. We intend to utilize optogenetics to test whether this striatal-pallidum microcircuit is capable of activating the auditory cortex.

Hypothesis: Stimulation of Jaws/inactivation of indirect striatal neurons will produce an effect analogous to enhanced dopamine activity on D_2 receptors and will result in increased c-Fos expression within the auditory cortex.

Methods: We have infused a retrograde AAV-Jaws/ChR2/GFP to express Jaws in 15 of our rats, Channelrhodopsin-2 (ChR2) in 6 of our rats, and GFP-only in 11 of our rats. After the optimal 6-week period of viral expression, the animals were surgically cannulated with fiber optics that permitted 630 nm light for AAV-Jaws and GFP-only groups and 470 nm light for AAV-ChR2 group. To ensure the rats did not dislodge the wireless optogenetic receiver during stimulation days, they were habituated with a dummy receiver for several days prior to days of stimulation. When stimulation day came, the rats were placed into a sound attenuated chamber and perfused 90 minutes afterwards to ensure optimal c-Fos expression from the optogenetic stimulation. The brains were extracted and immunohistochemically processed for c-Fos expression. These tissues were then imaged using fluorescent microscopy.

Results: Immunohistochemical analysis of the tissue for c-Fos expression showed significantly higher levels of c-Fos after stimulation of Jaws in indirect striatal neurons when compared to GFP-only and ChR2 groups. Animals transfected with ChR2 showed significantly less c-Fos expression when compared to Jaws but not GFP. Ipsilateral auditory cortex (Au1) with respect

to the viral infusion/fiber-optic placement showed significantly higher levels of c-Fos expression only in animals transfected with AAV-Jaws.

Conclusion: The results of this experiment suggests that the posterior caudatoputamen to lateral globus pallidus pathway is involved with auditory processes. Inhibiting this pathway with stimulation of Jaws was shown to significantly activate the primary auditory cortex when compared to the GFP control group. This supports our hypothesis that stimulation of Jaws within striatal neurons of the indirect pathway, analogous to dopamine inhibition via D_2 dopamine receptor activation, results in increased auditory cortex activity. In addition, we also confirmed the contrasting effect through the activation of striatal neurons within the indirect pathway via stimulation of ChR2 and observed no significant change in activity of the auditory cortex. We also observed significant ipsilateral activation of the Fiber-optic side of the auditory cortex when compared to the contralateral auditory cortex in the Jaws group. These findings bring our research closer to specifying a pathophysiological mechanism for auditory hallucinations.

3.2 Introduction

The basal ganglia comprise a group of subcortical nuclei that indirectly modulate various activities of the neocortex. The striatum is a subdivision of the basal ganglia that is the primary recipient of cortical input. The striatum can be divided into ventral and dorsal divisions; the dorsal division is comprised of the caudate nucleus and the putamen. Neurons of the dorsal striatum can be characterized as either direct, expressing predominantly D_1 dopamine receptors, or indirect, expressing D_2 dopamine receptors. These receptor subtypes are characterized by the G-protein subunits they activate and the net effect they have on intracellular cAMP in response to their activation by dopamine. In this regard, D_2 dopamine receptor neurons respond to dopamine by inhibiting adenylyl cyclase and decreasing intracellular cAMP, and conversely for D_1 receptor response to dopamine. Thus, the D_2 dopamine receptor neurons of the indirect pathway are generally inhibited by dopamine, even in the presence of glutamate input, while direct pathway neurons respond to dopamine in a converse manner (Gerfen and Surmeier, 2010).

Recent literature has focused on functional differentiation of the dorsal striatum. For example, the dorsal medial and dorsal lateral striatum have been functionally defined as executing goal-mediated and habitual behaviors, respectively (Alloway, 2017). Furthermore, a subregion of the dorsal striatum is involved with auditory processing and receives inputs from the auditory cortex

and medial geniculate body of the thalamus (Chen et al., 2019). These auditory cortex projections may function to tune auditory information for striatal sound representations. In addition, the posterior striatum may act to modulate sensory processing and cognitive aspects of the neocortex. Our laboratory has shown that dopamine infusion into a caudal (posterior) region of the caudatoputamen activates the rat auditory cortex in a pattern similar to that produced by sound. We believe that this provides a reasonable model of striatal involvement in regulation of auditory cortical activity, as might occur in schizophrenia. In addition, caudate volume has been determined to be strongly correlated with antipsychotic treatment response in patients with schizophrenia (Hutchenson, 2014).

An auditory hallucination is defined as the perception of a sound in a waking individual in the absence of an auditory stimulus (Blom, 2015). In the field of auditory hallucination research, there are many demarcations of the term to describe characteristics of the experience, e.g. auditory verbal/non-verbal hallucinations (Blom, 2015). Auditory hallucinations have been associated with a plethora of psychopathological states, including Parkinson's disease, major depression, and PTSD, and are a cardinal symptom of schizophrenia (Mørch-Johnsen, 2016; Baumeister et al., 2017; Frei & Truong, 2017). The association of the dorsal striatum with auditory hallucinations remains largely unexplored. The hallucinatory experience has largely been understood through phenomenological and functional neuroimaging studies, which reveal auditory cortical activation during hallucination (Lennox et al., 2000). However, the literature shows little agreement on the pathophysiology of hallucinations, and to our knowledge, none has addressed the relationship between auditory cortical activation and the striatal level. This study aims to elucidate a novel circuit that will establish a relationship between the auditory striatum and auditory cortical activation. The results of this study would translate into novel approaches to understand one of the core symptoms of psychosis.

3.3 Experimental Design

We utilized rAAV-induced gene transfer following infusion into the target region of LGP as identified in earlier experiments to retrogradely label indirect pathway neurons, respectively, with ChR2, Jaws or no opsin (GFP only). Expression of these viral constructs provided retrograde expression of opsins to either excite or inhibit labeled indirect striatal neurons. These opsins are sensitive to different wavelengths of light illumination from the fiber optic; ChR2 is sensitive to 470 nm blue light, while Jaws is sensitive to 630 nm red light. Rats received

stereotaxic intracranial infusion (1.0 µL) of rAAV-GFP-Ch2R, rAAV-GFP-Jaws or rAAV-GFP into the LGP, then animals recovered for at least 6 weeks to allow for retrograde transport and viral expression of opsin proteins in striatal cell bodies. Following this 6 week period, rats received an additional surgery to implant a fiber optic into the target region of striatum (the region retrogradely labeled by the earlier AAV infusion). The fiber optic, containing an LED of the prescribed wavelength, was attached to the skull with embedded screws and dental cement. Following recovery of at least 3 days, animals were habituated to handling. A dummy receiver (same weight as the wireless receiver) was attached to the fiber optic atop the head, and the rat was allowed to habituate to the weight of the receiver prior to the day of stimulations. On the experimental day, the wireless optogenetic receiver was attached to the fiber optic atop the head, and the rat was then transferred to the sound attenuated chamber (Startle/PPI chamber) with 70 dB white noise for 20 min of acclimation, this background noise assures equivalent auditory stimulation in all cases, and intermittent pulsatile/pseudo-continuous optogenetic stimulation for 30 min. After 90 min from start of stimulation, the rat was removed from the sound attenuated chamber, anesthetized, euthanized and perfused with 0.9% saline and 4% paraformaldehyde, with the brain removed for processing. Immunohistochemical labeling for c-Fos in serial sections through auditory cortex was imaged with fluorescent microscopy and analyzed with ImageJ Fiji automated cell counter. Labeling data was averaged from at least three adjacent sections to generate the mean labeling for that layer/region in that subject.

3.3.1 Animals and Virus

Subjects: This study consisted of 32 Sprague Dawley rats received from Charles river laboratory. These animals were separated in three cohorts: the first containing 6 animals transfected with 1.0 µL retro AAV-hSyn-GFP (#50465-AAVrg, addgene) with a viral titer of 7×10^{12} vg/mL and 6 transfected with 1.0 µL retro AAV-hSyn-Jaws-KGC-GFP-ER2 (#65014-AAVrg, addgene) with a viral titer of $1.3x10^{13}$ GC/mL, the second cohort contained 3 rats transfected with 0.1 µL retro AAV-hSyn-GFP, 3 rats transfected with 1.0 µL AAV-hSyn-Jaws-KGC-GFP-ER2 and 6 rats transfected with 1.0 µL retro AAV-Syn-ChR2(H134R)-GFP (#58880-AAVrg, addgene) at viral titer of $7.4x10^{12}$ GC/mL and the third cohort contained 6 more in the retro AAV-hSyn-Jaws-KGC-GFP-ER2 group and two more in the retro AAV-hSyn-GFP group. The operating weight for viral infusions was maintained at 250 grams, this would ensure the most accuracy when referencing the stereotactic coordinates from the Paxinos and Watson atlas. After 6-week optimal retroviral expression of opsins/fusion proteins, rats weighed on

average 450 grams for initial fiber optic implant surgeries. Rats were also group-housed in a controlled environment with a 12-hour reverse light/dark cycle housing (lights on from 9PM-9AM). Food and water were available *ad libitum*. These experiments were all approved by the University of Arizona Institute of Animal Care and Use Committee

3.3.2 *In vivo* optogenetic stimulation setup

Habituation periods started on the third day following fiber optic implant surgery. These days consisted of habituating the rats to a 2g Teleopto dummy receiver for 30 minutes up until the day of stimulation. On test day, a 2 g Teleopto wireless receiver was connected to the fiber optic atop the headmount. An IR remote emitter inside the sound attenuated chamber allowed for direct control of the receiver by TTL pulses from a programmable stimulator (located outside the chamber), providing ~10 mW of light output at the tip of the fiber optic. 70-dB white noise was constant throughout the period in the sound attenuated chamber. This background noise provided consistent sound throughout stimulation and also the attenuation of less controlled noises outside the stimulation room.

3.3.3 Surgeries: Craniotomy and Fiberoptic implantation

To prepare animals for surgical procedures, they were first anesthetized briefly in an isoflurane chamber. After brief anesthetization, the surgical site on the head was shaved and cleaned and the subjects were fitted to the Kopf stereotactic frame. The subjects were then fitted with a nasal piece that delivered continuous supply of 2-4% isoflurane. Each subject was administered a 1mg/kg dose of meloxicam (Alloxate) for post-surgical analgesia. Ipsilateral craniotomies were achieved with a drill which produced a 0.2 mm hole in the skull at the site of viral infusion, lateral globus pallidus (-1.8 mm AP, +3.9 mm ML, -6.0 mm DV), or fiber optic implantation, posterior caudatoputamen (-1.8 mm AP, +4.4mm ML, -4.8 mm DV). After viral infusions, the skull was cleaned, and the craniotomy was sealed with bone wax. Viral infusions were delivered with a 5μL Hamiltonian syringe. The incision site was closed with suture (Coated Vicryl 4-0 undyed braided suture, Ethicon) and lidocaine gel was applied followed by a triple antibiotic gel. For fiber optic surgeries, the fiber was placed in the 0.2 mm hole in the skull and sealed with acrylic cement (Ortho-Jet BCA powder, REF B1330, Lang Dental Manufacturing Co.). The headmount produced from the acrylic cement was fitted with two paperclips placed

orthogonal to each other. This allowed for a surface that was used to secure the Teleopto wireless optogenetic receiver to the headmount.

3.3.4 Euthanasia of animals

Animals were euthanized after receiving intraperitoneal injection with Euthasol sodium pentobarbital (200 mg/kg, i.p.) and by transcardial perfusion with 4% paraformaldehyde (0.9% NaCl) for tissue fixation in histochemical studies. These euthanasia methods are consistent with recommendations of the American Veterinary Medical Association Panel on Euthanasia.

3.3.5 Tissue processing and Immunohistochemical analysis

After extracted brains have settled for 90 minutes in 4% paraformaldehyde, brains were then treated with 12.5% (24 hours) and 25.0% sucrose gradients until tissue freezing. Brains were then immersed in O.C.T (optimal cutting tissue) medium followed by snap freezing in crushed/powered dry ice. These brains are then sectioned by the Leica CM195 Cryostat and collected on microscope slides which are vacuum dried for 10 minutes prior to being stored in 4°C freezer overnight. Long term slide storage was kept in a -80°C freezer until immunohistochemical analysis is required.

Immunohistochemistry processes involved staining for the transcription factor c-Fos. Slides were washed three times for 5 minutes in 0.05M KPBS buffer solution before and after each incubation period. Tissue was blocked with 5% Normal Goat Serum (NGS) solution made from 0.05M KPBS (pH = 7.4) and 0.4% Triton X-100 for 1-hour. Afterwards, the tissue was incubated with the primary antibody, c-Fos Rabbit mAB (cell signaling, #2250), at 1:2400 dilution with 10% NGS (0.05 KPBS, 0.4% TX) for 48-hours. After this incubation period, the slides were then incubated with Alexa Fluor-594 goat anti-rabbit IgG secondary antibody (Invitrogen, R37117) for a period of 45-minutes. Once this incubation was complete, slides were then coverslipped with ProLong™ Diamond Antifade Mountant (Invitrogen, P36970). Immunofluorescence was captured using the Zeiss Axio Imager M2 upright widefield fluorescent microscope and the Zen image analysis software. ImageJ with Fiji was used to count cells labeled with c-Fos. Scale bars were converted from 2.25 µm/pixel for 5x images and 0.9 µm/pixel for 10x images.

3.3.6 Statistical analysis and mathematical equations

Three 20µm sections from each animal within the same approximate region of the primary auditory cortex (-4.3 mm A/P) were analyzed with ImageJ Fiji via automated cell counts. The parameters used for the automated cell counts are 0.5-1.0 circularity, 30-255 threshold and 100-10000 pixel cell area. The approximate size of the region for cellular analysis of the auditory cortex is $4mm^2$. Immunohistochemical data was analyzed via parametric statistical tests with one-way ANOVA, followed by Tukey's multiple comparison test of optogenetic stimulation and two-way ANOVA followed by Sidak's multiple comparison tests for ipsilateral/contralateral c-Fos expression in optogenetically stimulated brains. Statistical significance was determined if the resulting p values ≤ 0.05.

3.4 Results

3.4.1 Infusion sites LGP-CPu microcircuit

The results of our first experiment showed us that the lateral globus pallidus (LGP), at the same rostral-caudal level (-1.8 mm AP) as the infusion site in the caudatoputamen (CPu), is the main projecting site of the posterior CPu. Because of this result, we decided to infuse the retrograde adeno-associated virus with associated opsins into this region of the LGP (Figure 9). This allowed for the expression of the associated opsin (i.e. ChR2 or Jaws) to be primarily in the posterior CPu region of the auditory striatum.

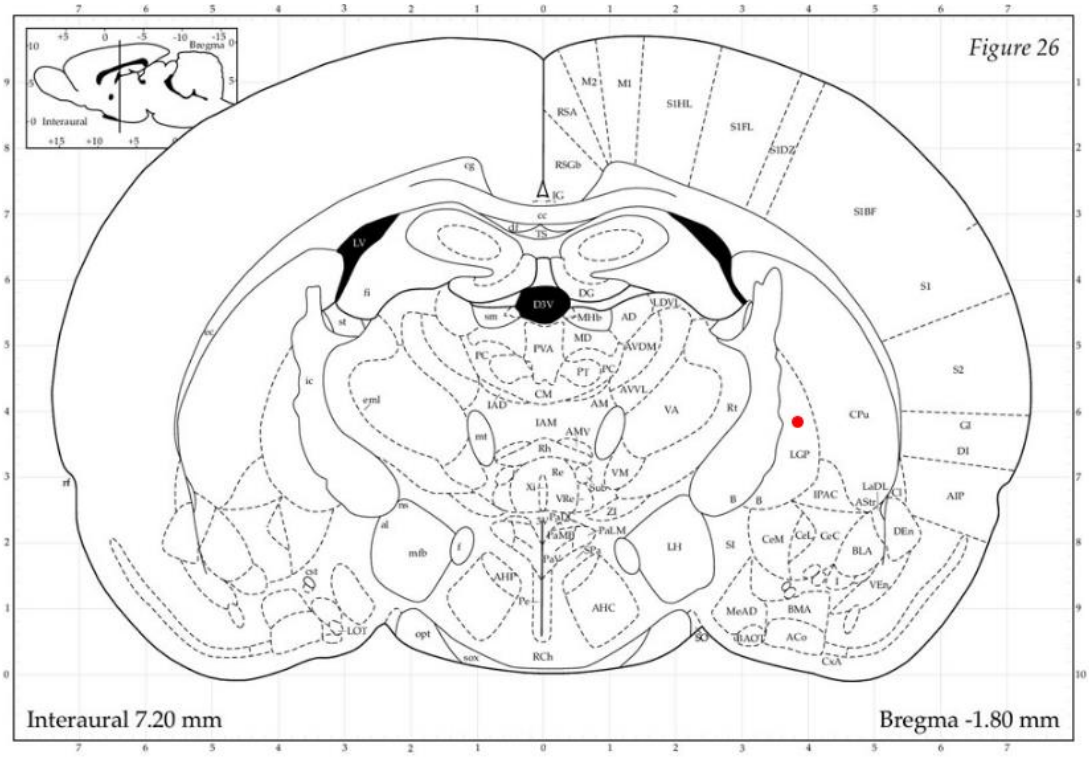

Figure 9. Illustrates the target infusion site of retrograde AAVs with the Paxinos and Watson stereotaxic coordinate atlas 2006 edition. The red dot is marked with the following coordinates (-1.8mm AP, +3.9mm ML, -6.2mm DV, 0^0 tilt). Gaidica, M. (2019). Rat Brain Atlas. Retrieved 16 December 2019, from http://labs.gaidi.ca/rat-brain-atlas/

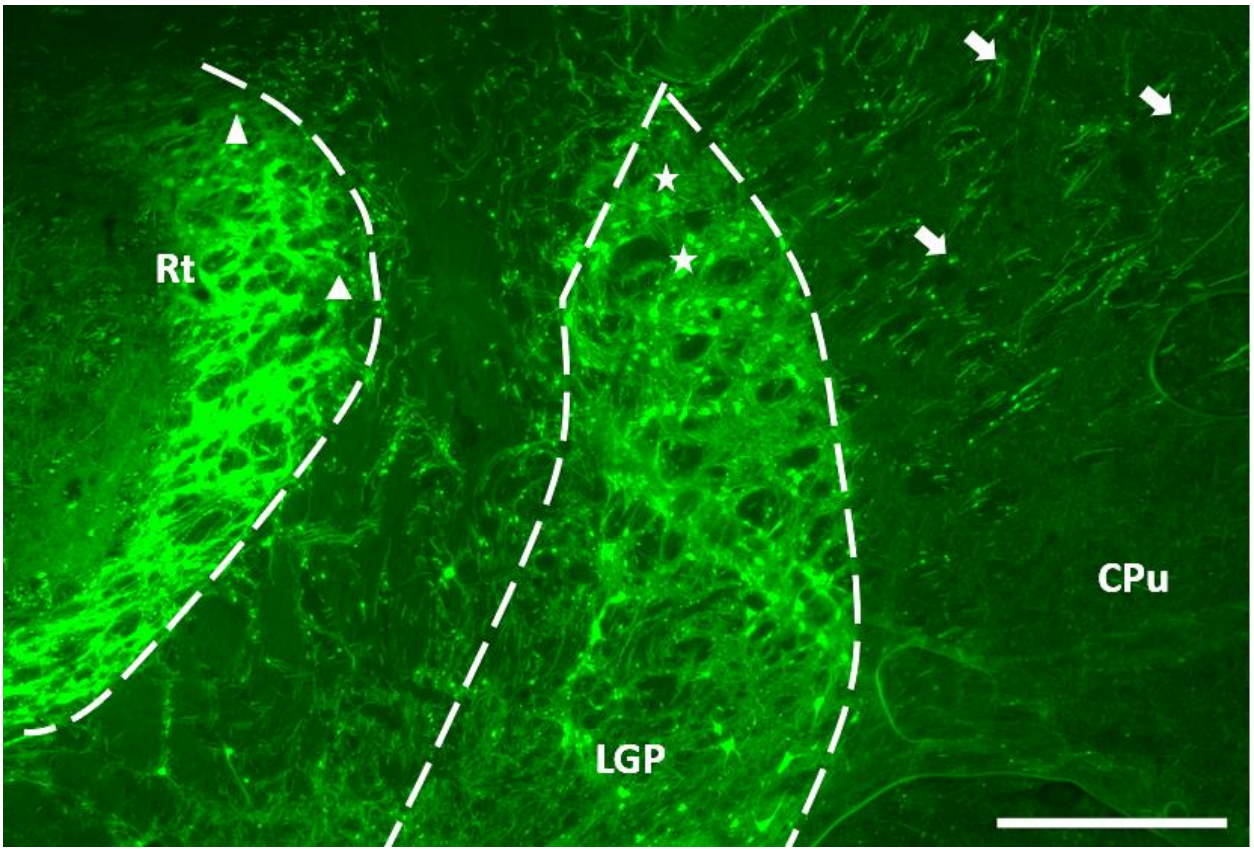

Figure 10. Expression of the retrograde AAV-hSyn-eGFP was observed in the reticular thalamus (RT), lateral globus pallidus (LGP) and the caudatoputamen (CPu). Triangles indicate cell body labeling in the Rt. Stars indicate labeling in the LGP-CPu border region. Arrows indicate cells labeled in the lateral aspect of the CPu. Scale bar is 1000 µm.

Viral infusion into the LGP (-1.8mm AP, +3.9mm ML, -6.2mm DV) with retrograde Adeno-associated viruses and their respected opsins, resulted in labeling of the reticular thalamus and lateral caudatoputamen border near the LGP (Figure 10). As depicted in Figure 11, this trend was observed in all retrograde viruses. However, the exact demarcation of the LGP-CPu border is uncertain. Though we are certain that LGP retroviral infusion resulted in CPu labeling not just around this border, but sparse amounts are shown throughout CPu (Figure 10).

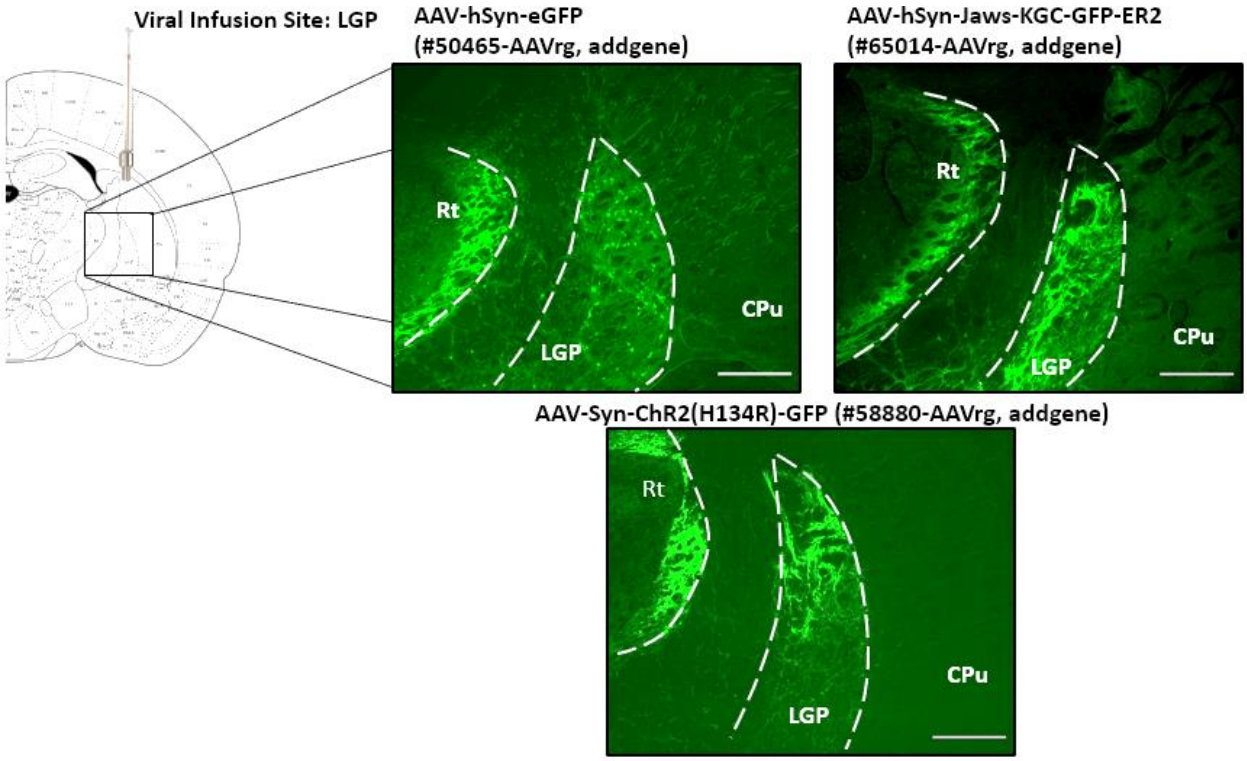

Figure 11. Illustrates viral GFP expression mainly in the lateral globus pallidus (LGP), reticular thalamus (Rt) and minor expression in the caudatoputamen (CPu). Scale bar is 1000 μm

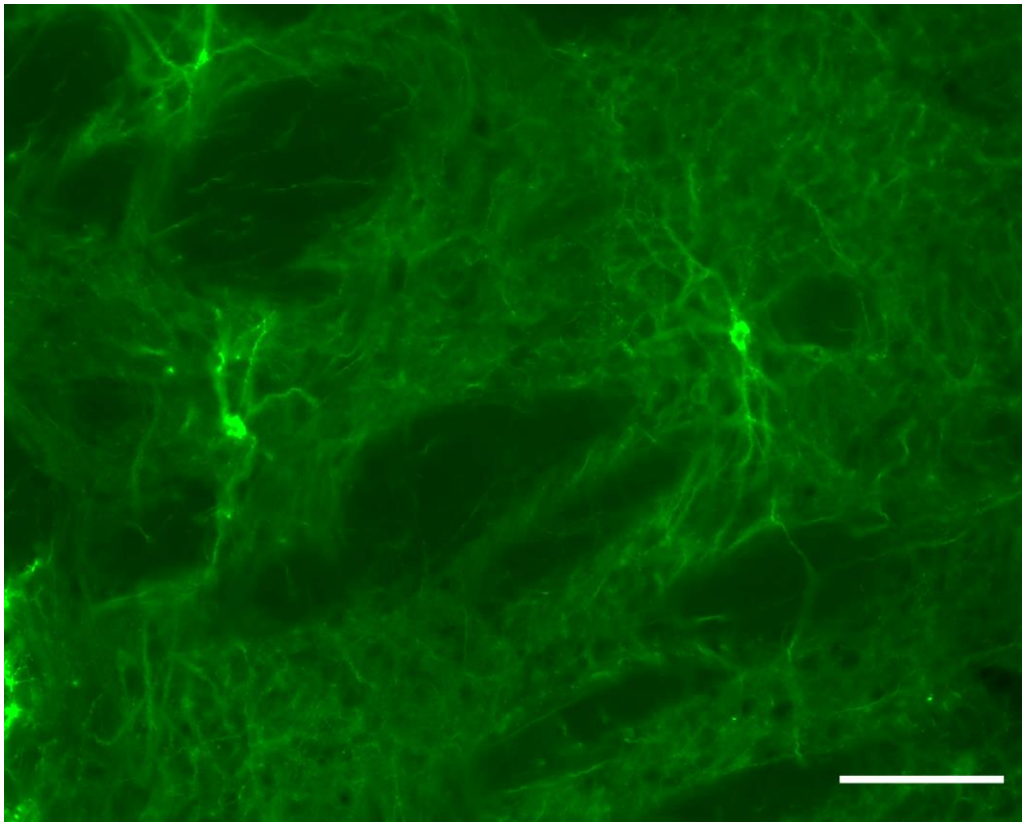

Figure 12. Magnified image of Striatal neurons of caudatoputamen transfected with AAV-hSyn-Jaws-KGC-GFP-ER2.

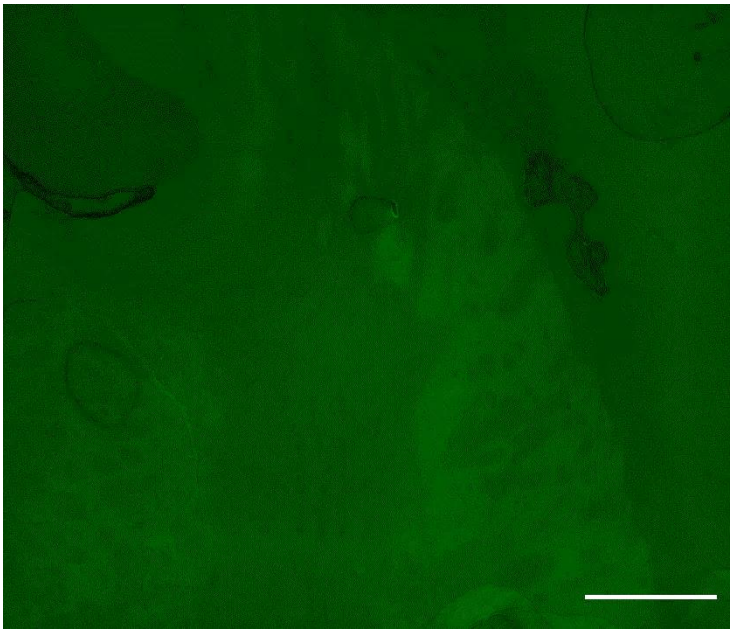

Figure 13. Example of excluded brain from c-Fos analysis due to no GFP expression in CPu.

3.4.2 Optogenetic stimulation of indirect pathway

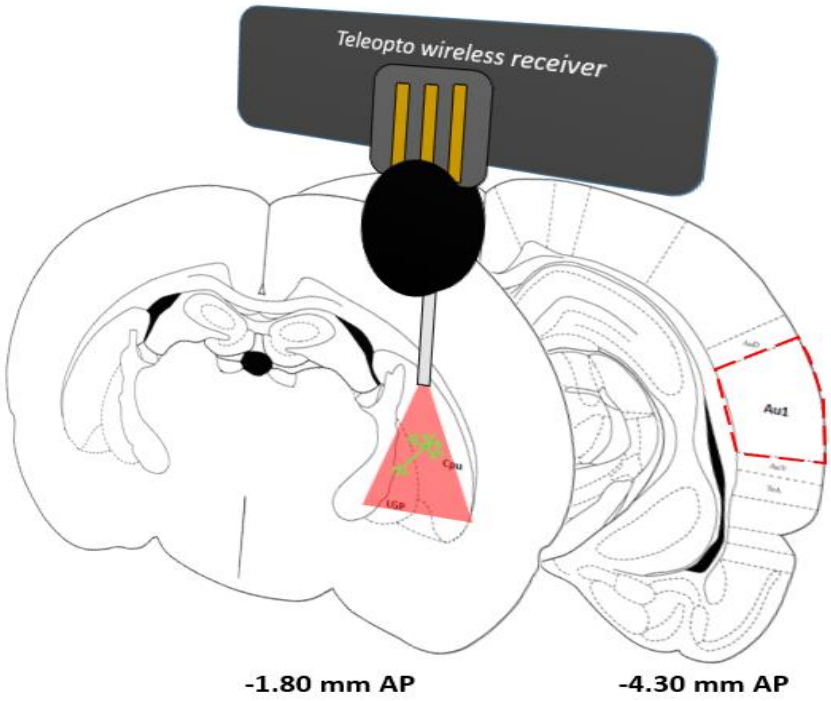

Figure 14. Illustration of Fiber optic stimulation paradigm. Including the region of stimulation CPu-GP microcircuit (-1.8 mm AP) and the region of expected activation primary auditory cortex (Au1, -4.30 mm AP). Illustration depicts the unilateral fiber optic stimulation with 630nm red light of the CPu-GP.

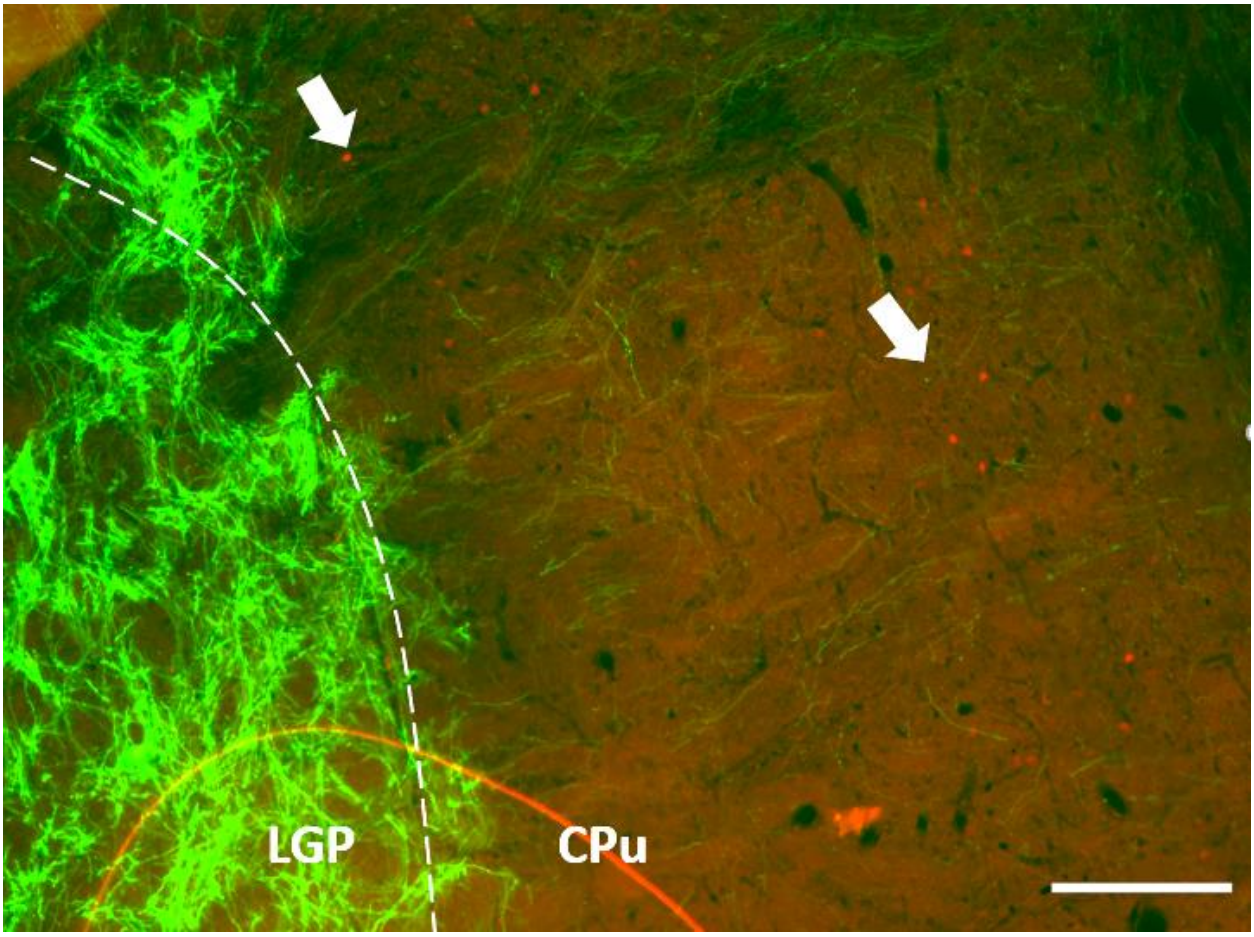

Figure 15. Expression of c-Fos in the posterior caudatoputamen of brain transfected with retrograde AAV-Syn-ChR2(H134R)-GFP in LGP. Scale bar 500µm.

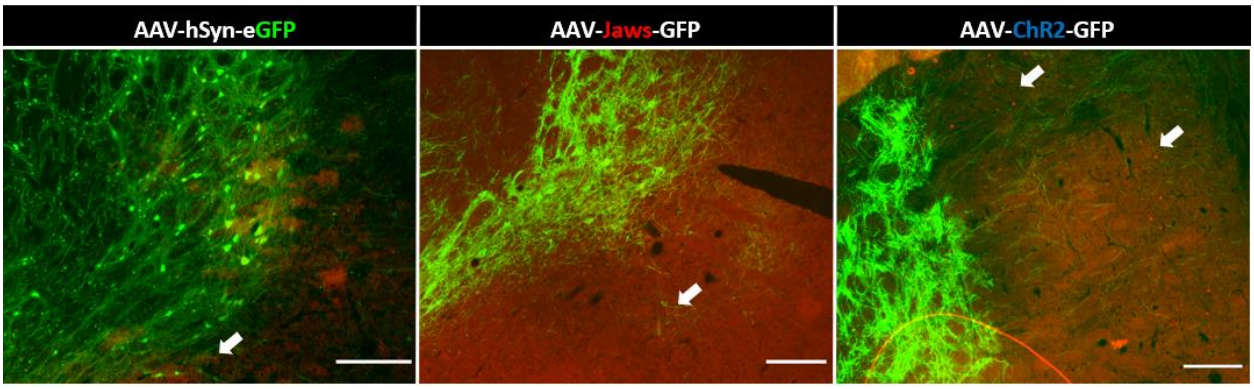

Figure 16. Expression of c-Fos in posterior caudatoputamen of all groups. White arrows depict c-fos expression. Scale bar 500µm.

Stimulation of caudatoputamen region near fiber optic placement (-1.8mm A/P, +4.4mm M/L, -4.8mm D/V, 0^0 tilt) resulted in sparse c-Fos expression in rats transfected with AAV-GFP-only and AAV-Jaws (Figure 16). However, those transfected with AAV-ChR2 appeared to have more c-Fos labeling in striatum (Figure 15). The c-Fos expression in AAV-ChR2 brains was also more pronounced and easily recognized when compared to the AAV-GFP-only and AAV-Jaws.

3.4.3 Images of Au1 and analysis of c-Fos

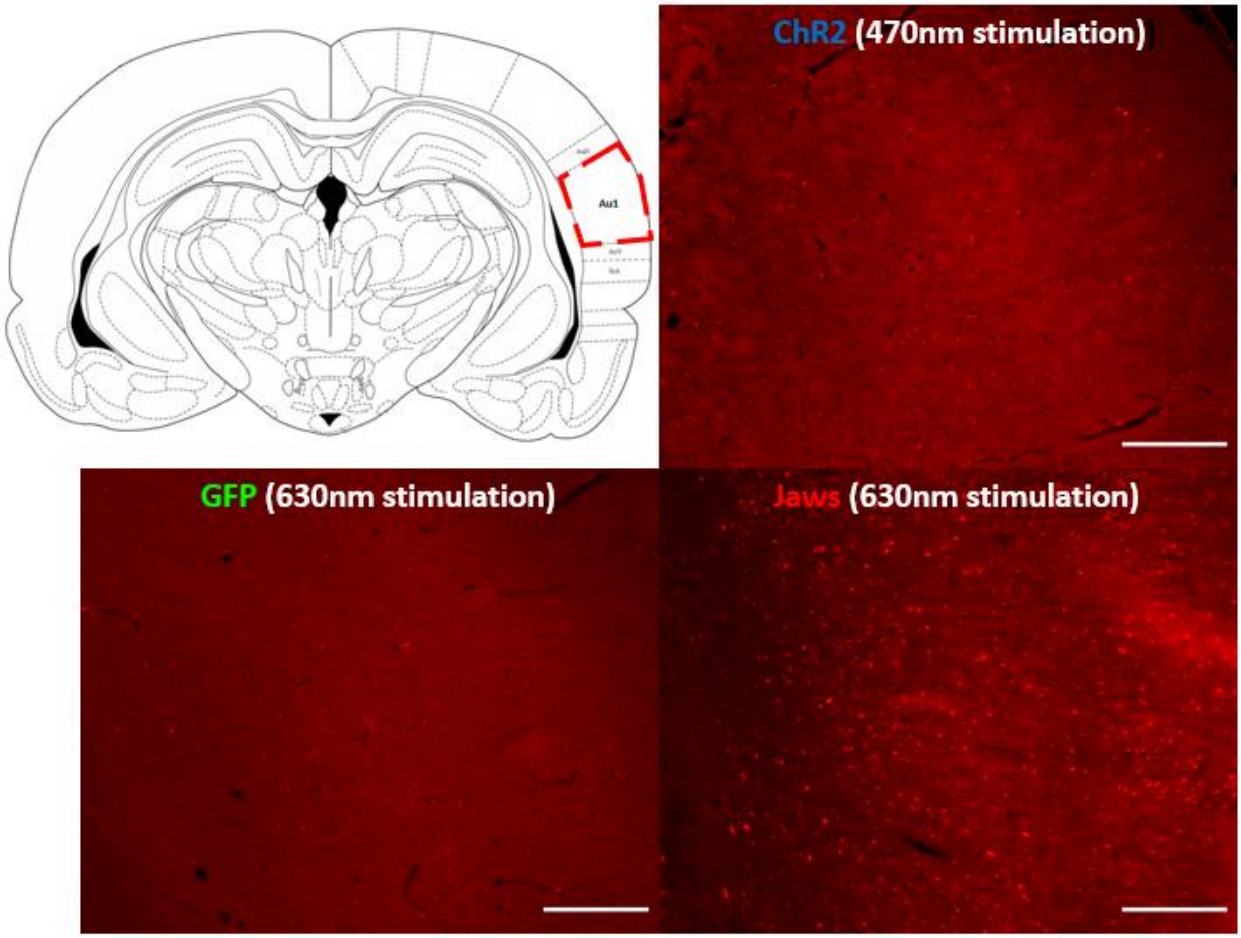

Figure 17. Images depict the various levels of c-Fos expression in primary auditory cortex (Au1) of brains either expressing GFP-only, Jaws or ChR2, at approximately -4.3mm A/P in the Paxinos and Watson 2006 Stereotaxic atlas. Region of analysis for c-Fos was calculated to be roughly 4 mm^2. Scale bar 500μm.

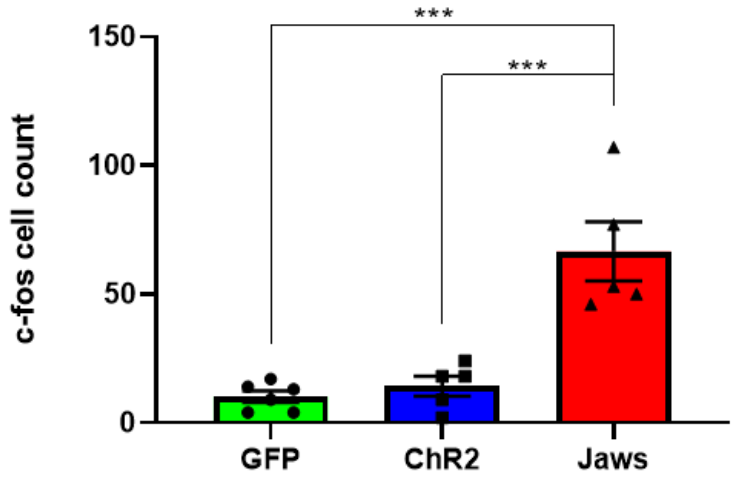

Figure 18. Depicts c-Fos cell counts of Au1 for brains containing GFP-only, ChR2, and Jaws when stimulated with appropriate wavelengths of light. *** p-value <0.001.

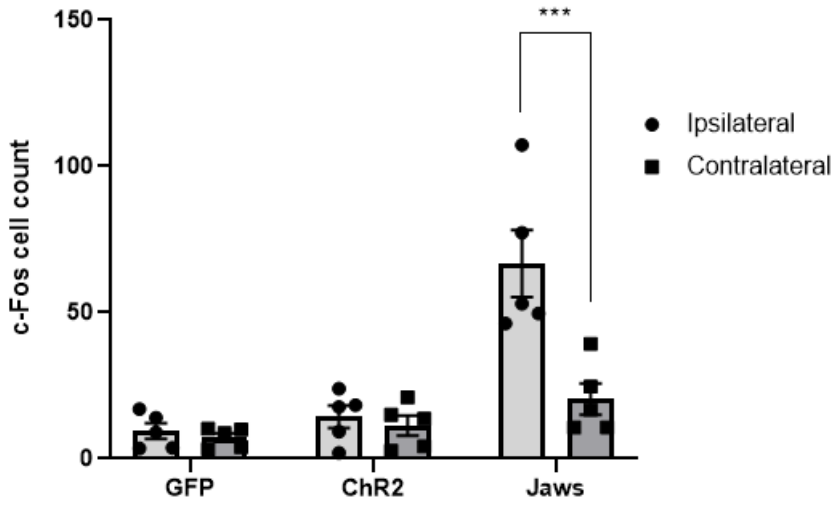

Figure 19. Comparison of c-Fos cell counts of ipsilateral/contralateral Au1 regions respective to fiber optic placement. *** p-value <0.001.

		c-Fos cell counts									
		Ipsilateral Au1				Contralateral Au1					
	Virus	S1	S2	S3	Ave	S1	S2	S3	Ave		
2R1(GFP)	GFP	4	3	3	**3.5**	2	4	4	**3.3**		
2R2(GFP)	GFP	8	15	28	**17**	9	7	10	**8.7**		
2R3(GFP)	GFP	3	5	3	**3.7**	5	0	7	**4.0**		
R3 (GFP)	GFP	13	15	14	**14**	15	7	9	**10.3**		
R4 (GFP)	GFP	12	8	7	**9**	10	12	8	**10**		
R12(GFP)	GFP	18	12	8	**12.7**	12	13	9	**11.3**		
2R7(CHR2)	CHR2	23	25	24	**24**	21	11	31	**21**		
2R9(CHR2)	CHR2	11	18	24	**17.7**	2	6	5	**4.3**		
2R10(CHR2)	CHR2	11	5	12	**9.3**	14	20	11	**15**		
2R11(CHR2)	CHR2	4	34	17	**18.3**	16	7	18	**13.7**		
2R12(CHR2)	CHR2	0	4	2	**2**	1	5	2	**2. 7**		
R10(JAWS)	JAWS	33	37	79	**49.7**	8	45	21	**24.7**		
R11(JAWS)	JAWS	76	76	80	**77.3**	36	53	29	**39.3**		
2R5(JAWS)	JAWS	118	105	99	**107.3**	13	20	17	**16.7**		
2R6	JAWS	47	45	47	**46.3**	16	7	9	**10.7**		
R1	JAWS	54	61	44	**53**	11	8	13	**10.7**		
Automated cell requirements	Circularity measure	Cell-size exclusion	Area of analysis	threshold							
	0.5-1.0	100-100k	~4 mm^2	30-255							
Statistical summaries	One-way ANOVA Tukey's multiple comparison test			Two-way ANOVA Sidak's multiple comparisons test							
GFP vs. ChR2	p-value = 0.9025										
GFP vs. Jaws	**p-value = 0.0001**										
Jaws vs ChR2	**p-value = 0.0003**										
Jaws ipsilateral vs Jaws contralateral				**p-value = 0.0001**							

Table 2. c-Fos cell counts and statistical analysis summaries. Excluded animals either did not meet the criteria for expression of GFP in caudatoputamen or were euthanized due to complications of surgery/infection.

Stimulation of Jaws within striatal neurons of the indirect pathway resulted in the highest c-Fos cell counts in the primary auditory cortex (Au1) when compared to other groups (ChR2 and GFP). One-way ANOVA with Tukey's multiple comparisons test (Table 2) showed that the only

observed significant difference between groups was that of Jaws vs. GFP (p-value = 0.0001) and Jaws vs. ChR2 (p-value = 0.0003). There were no significant differences between ChR2 vs. GFP (p-value = 0.9025). Comparing the c-Fos counts between ipsilateral to contralateral regions of Au1 respective to fiberoptic placement showed significant differences only in Jaws group (p-value = 0.0001).

3.5 Discussion

Traditionally the basal ganglia were solely the focus of motor behavior and the target of motor-related diseases (Galvin & Smith, 2010). However, recent studies have suggested several sensory processing pathways of the posterior striatum. These studies have shown that visual- and auditory-striatal subdivisions exist in the caudal regions of the dorsal striatum (Seger, 2013) of human and rodent brains. Even more recently, mouse studies have shown auditory sensory thalamus (Medial geniculate body of thalamus) and primary auditory cortex both project to an "auditory striatum" (Chen et al, 2019). Each of these projections to the posterior striatum carry unique auditory information as silencing either one of their projections impairs auditory frequency discrimination in specific frequency ranges (Chen et al, 2019). However, none of these studies, however, have examined the cortical-striato-pallido-thalamo-cortical pathway of auditory cortical activation mediated via the level of striatal-pallidal indirect pathway.

Anatomical discrimination of the indirect pathway was accomplished in our tracer study, and the precise region of lateral globus pallidus (LGP; indirect pathway terminals) was determined. This region of the lateral globus pallidus was then targeted with a retrograde adeno-associated virus expressing the desired opsin (Jaws or ChR2) in the posterior striatum of rats (CPu, -1.8 mm A/P). We also showed previously that neurons expressing Jaws could be sufficiently activated with 3s pulse at 0.3Hz (parameter B). These results were then used to inactivate neurons of the indirect pathway with Jaws and also activate neurons of the direct pathway with ChR2. What we found was a significant c-Fos response in the primary auditory cortex (Au1, -4.3 mm A/P) with 630nm stimulation of Jaws with 3s pulse at 0.3Hz in the posterior striatum (-1.8mm AP, +3.9mm ML, -4.8mm DV). There was no significant c-Fos response in the primary auditory cortex when 470nm stimulation of ChR2 was applied at 15ms pulse 10Hz in the posterior striatum. Ipsilateral expression of c-Fos in primary auditory cortex was significantly higher than contralateral expression only in animals stimulated with Jaws (p-value<0.001). We conclude that the

caudatoputamen to lateral globus pallidus neurons in rats contains auditory information and follows aspects of the canonical basal ganglia signaling.

It is well known to researchers studying positive symptoms of schizophrenia how notoriously difficult it is to model these states. The most commonly used model for positive symptoms has been D_2 receptor hyperactivity in the striatum (Canetta & Kallendonk, 2018). The aforementioned model has been used to depict correlations between enhanced striatal dopamine and the severity of positive symptoms. Our results illustrate a specified region of the posterior striatum in rodents that's likely responsible for the positive symptoms experienced as a result of enhanced striatal dopamine. Therefore, our findings further specify and enhance future models aimed at explaining the pathophysiology of the positive symptoms of schizophrenia.

CHAPTER 4

DISCUSSION

In our experiments we have approached the cortio-striatal-pallidal-thalamo-cortical (CSPTC) loops, that have been more traditionally focused on motor related diseases, with the ideal of elucidating a mechanism for auditory cortical activation at the striatal level. Previous studies done within our lab have shown that dopamine infusions in this posterior region of the rodent striatum (CPu) are capable of eliciting activation of auditory cortex (Au1) (Parga, Zafar, Nikulina & Hammer, 2019). We know that this result is likely from dopamine's effect on D_2 receptors, reducing cAMP via inhibition of adenylyl cyclase, causing disinhibition of thalamic nuclei via deactivation of external globus pallidus (Figure 1). The dopamine hypothesis has been a long standing, continuously evolving theory for explaining symptoms of psychosis (Howes & Kapur, 2009). Hyperdopaminergic states in the striatum have been correlated to symptoms of psychosis, such as auditory hallucinations (Howes & Kapur, 2009). This knowledge and prior experimenting led us to believe that there is a posterior region of the striatum capable of processing auditory information, and its ability to induce auditory hallucinations (activation) is contingent on indirect pathway activity at the striatal-pallidal level. This would provide a novel approach for understanding the role of striatal pathophysiology in auditory hallucinations.

Though we knew that dopamine infusions into the posterior caudatoputamen (-1.8mm A/P, +4.4mm M/L, -6.0mm D/V, 0^0 tilt) was able to activate the auditory cortex, and that this was likely through D_2 receptor activation on indirect neurons, we were unsure of where in the lateral globus pallidus that these striatal neurons projected to. Utilizing an anterograde adeno-associated virus, infusing at the same point of the dopamine infusions, we found that terminals mainly projected to the LGP at the same rostral-caudal level as viral infusion site (-1.8mm A/P). This result allowed us to target the same striatal neurons with virally expressed opsins (Jaws and ChR2). However, we knew from previous studies that ChR2 is effective at stimulating neurons with 15ms pulses at 10Hz, but we were unsure of what parameters would be effective with Jaws. Boyden's lab did a thorough analysis on the Jaws opsin and found that continuous parameters were best when inactivating neurons with Jaws (Chuong et al., 2014). Therefore, we developed two pseudo-continuous parameters (8s pulse 0.1 Hz and 3s pulse 0.3Hz) that would work with our experiment and ran a preliminary study to test them. We transfected rats with retrograde AAV-Jaws-GFP into a motor region of the LGP-CPu microcircuit (-1.0mm A/P, +2.9mm M/L, -6.0mm D/V, 0^0). We hypothesized that inhibiting this circuit would activate motor

cortices and we would compare the amount of c-Fos expression as a level of the parameter's effectiveness. There was no significant difference (n=1, p-value=0.1314) in the amount of c-Fos expression. In spite of this, qualitative analysis of the c-Fos expression showed better results for 3s pulse at 0.3Hz when activating the motor cortices. Therefore, we decided to use this parameter for our future studies involving Jaws.

Utilizing the LGP coordinates (-1.8mm A/P, +3.9mm M/L, -6.2mm D/V, 0^0 tilt) we virally infused retroactive adeno-associated viruses with Jaws into the LGP and retrogradely expressed Jaws into striatal indirect neurons. Stimulation of these neurons with 630nm red-light with 3s pulse at 0.3Hz produced c-Fos expression in the primary auditory cortex that was significantly greater than those of retrograde AAV-hSyn-GFP brains (n=6, p-value =0.0001) and also brains stimulated with 470nm blue-light that were transfected with retrograde AAV-ChR2(H134r)-GFP (n=5, p-value=0.0003). We also compared the ipsilateral and contralateral primary auditory cortices with respect to fiber optic probe and found that Jaws inactivation of striatal-pallidal neurons resulted in significantly greater amounts of ipsilateral expression of c-Fos (n=5, p-value=0.0001). This result is consistent with experiments that showed activation of unilateral auditory cortex in mice with picrotoxin infusions only resulted in ipsilateral Fos expression in caudal striatum (Arnauld et al., 1996). Therefore, our results complement the notion of a topographical organization of cortico-striatal-pallidal-thalamo-cortical connections that process auditory information.

4.1 Conclusion

The results from our experiments are critical findings, as recent literature has yet to associate the functional significance of D_2 receptor expressing indirect pathway striatal neurons of posterior striatum with the perception of sound. I believe our results show the significance of a striatal-pallidal microcircuit that can be further established to model auditory hallucinations experienced by sufferers with schizophrenia. These results provide for an understanding of the role of striatal pathophysiology in regard to auditory hallucinations. This is not only a result that can further refine our models of schizophrenia for research but also potentially improve targeted therapeutics for those suffering from the symptoms of psychosis.

4.2 Future studies

From the results of our experiments we know that a striatal-pallidal indirect pathway microcircuit capable of activating the auditory cortex exists. However, we do not know specifically how this pathway contributes to the experience of the positive symptoms of schizophrenia. At this point, we are left to speculate whether it is the pathway responsible for internally generated sound processes or something else. I propose future experiments which aim towards establishing this pathway's function in regard to sensorimotor gating. We know from cross-sectional studies that Prepulse inhibition (PPI) is an effective biomarker for acute and chronic sufferers of schizophrenia (Mena et al., 2016). It would be interesting to see how this striatal-pallidal indirect pathway would affect Prepulse inhibition in rats. I speculate that inhibition of this microcircuit would result in reduced PPI in rats, analogous to reduced PPI seen in those suffering from schizophrenia.

REFERENCES

Allen, P., Larøi, F., McGuire, P. K., & Aleman, A. (2008). *The hallucinating brain: A review of structural and functional neuroimaging studies of hallucinations. Neuroscience & Biobehavioral Reviews, **32**(1), 175–191.*

Alloway, K. D., Smith, J. B., Mowery, T. M., & Watson, G. D. R. (2017). Sensory Processing in the Dorsolateral Striatum: The Contribution of Thalamostriatal Pathways. Frontiers in Systems Neuroscience, **11**.

Arenkiel, B. R., Peca, J., Davison, I. G., Feliciano, C., Deisseroth, K., Augustine, G. J., … Feng, G. (2007). In vivo light-induced activation of neural circuitry in transgenic mice expressing channelrhodopsin-2. *Neuron*, ***54***(2), 205–218.

Baumeister, D., Sedgwick, O., Howes, O., & Peters, E. (2017). Auditory verbal hallucinations and continuum models of psychosis: A systematic review of the healthy voice-hearer literature. Clinical Psychology Review, **51**, 125–141.

Blom, J. D. (2015). Auditory hallucinations. Handbook of Clinical Neurology, 433–455.

Blom, J. D., Looijestijn, J., Goekoop, R., Diederen, K. M. J., Rijkaart, A.-M., Slotema, C. W., & Sommer, I. E. C. (2011). *Treatment of Alice in Wonderland Syndrome and Verbal Auditory Hallucinations Using Repetitive Transcranial Magnetic Stimulation: A Case Report with fMRI Findings. Psychopathology, 44(5), 337–344.*

Bohlken, M. M., Hugdahl, K., & Sommer, I. E. C. (2016). *Auditory verbal hallucinations: neuroimaging and treatment. Psychological Medicine, **47**(02), 199–208.*

Britt, J. P., McDevitt, R. A., & Bonci, A. (2012). Use of channelrhodopsin for activation of CNS neurons. *Current protocols in neuroscience*, *Chapter 2*, Unit2.16.

Canetta, S., & Kellendonk, C. (2018). *Can we use mice to study schizophrenia? Philosophical Transactions of the Royal Society B: Biological Sciences, 373(1742)*

Chen, L., Wang, X., Ge, S., & Xiong, Q. (2019). Medial geniculate body and primary auditory cortex differentially contribute to striatal sound representations. *Nature communications*, ***10***(1), 418.

Chung, L. (2015). *A Brief Introduction to the Transduction of Neural Activity into Fos Signal. Development & Reproduction, **19**(2), 61–67*

Chuong, A. S., Miri, M. L., Busskamp, V., Matthews, G. A., Acker, L. C., Sørensen, A. T., … Boyden, E. S. (2014). Noninvasive optical inhibition with a red-shifted microbial rhodopsin. *Nature neuroscience*, ***17***(8), 1123–1129.

Curran,T. A., Miller, D., Zokas, L., & Verma, I. M. (1984). *Viral and cellular fos proteins: A comparative analysis. Cell, **36**(2), 259–268.*

Freeze, B. S., Kravitz, A. V., Hammack, N., Berke, J. D., & Kreitzer, A. C. (2013). Control of Basal Ganglia Output by Direct and Indirect Pathway Projection Neurons. Journal of Neuroscience, **33**(47), 18531–18539.

Frei, K., & Truong, D. D. (2017). Hallucinations and the spectrum of psychosis in Parkinson's disease. Journal of the Neurological Sciences, **374**, 56–62.

Gerfen, C. R. and D. J. Surmeier (2010). Modulation of striatal projection systems by dopamine. Annual review of neuroscience. July, 2010.

González-Maeso, J., Weisstaub, N. V., Zhou, M., Chan, P., Ivic, L., Ang, R., … Gingrich, J. A. (2007). *Hallucinogens Recruit Specific Cortical 5-HT2A Receptor-Mediated Signaling Pathways to Affect Behavior. Neuron, **53**(3), 439–452.*

González-Maeso, J., & Sealfon, S. C. (2009). *Psychedelics and schizophrenia. Trends in Neurosciences, **32**(4), 225–232.*

Guo, L., Walker, W. I., Ponvert, N. D., Penix, P. L., & Jaramillo, S. (2018). Stable representation of sounds in the posterior striatum during flexible auditory decisions. *Nature communications*, ***9***(1), 1534.

Guru, A., Post, R. J., Ho, Y. Y., & Warden, M. R. (2015). Making Sense of Optogenetics. *The international journal of neuropsychopharmacology*, *18*(11)

Horga, G., Parellada, E., Lomeña, F., Fernández-Egea, E., Mané, A., Font, M., … Bernardo, M. (2011). Differential brain glucose metabolic patterns in antipsychotic-naïve first-episode schizophrenia with and without auditory verbal hallucinations. *Journal of psychiatry & neuroscience : JPN*, ***36***(5), 312–321.

Howes, O. D., & Kapur, S. (2009). *The Dopamine Hypothesis of Schizophrenia: Version III--The Final Common Pathway. Schizophrenia Bulletin, **35**(3), 549–562.*

Hunnicutt, B. J., Jongbloets, B. C., Birdsong, W. T., Gertz, K. J., Zhong, H., & Mao, T. (2016). A comprehensive excitatory input map of the striatum reveals novel functional organization. *eLife*, ***5***, e19103.

Hutcheson, N. L., Clark, D. G., Bolding, M. S., White, D. M., & Lahti, A. C. (2014). *Basal ganglia volume in unmedicated patients with schizophrenia is associated with treatment response to antipsychotic medication. Psychiatry Research: Neuroimaging, **221**(1), 6–12.*

Javitt, D. C., & Sweet, R. A. (2015). Auditory dysfunction in schizophrenia: integrating clinical and basic features. *Nature reviews. Neuroscience*, ***16***(9), 535–550

Javitt, D. C., & Zukin, S. R. (1991). Recent advances in the phencyclidine model of schizophrenia. *American Journal of Psychiatry, **148**(10), 1301–1308.* doi:10.1176/ajp.148.10.1301

Lennox, B. R., Park, S.B., Medley, I., Morris, P. G. & Jones, P. B. (2000). The functional anatomy of auditory hallucinations in schizophrenia. Psychiatry Res **100**(1): 13-20.

Levitan, C., Ward, P. B., & Catts, S. V. (1999). *Superior temporal gyral volumes and laterality correlates of auditory hallucinations in schizophrenia. Biological Psychiatry, 46(7), 955–962.*

Lin J. Y. (2011). A user's guide to channelrhodopsin variants: features, limitations and future developments. Experimental physiology, **96**(1), 19–25.

Mørch-Johnsen, L., Nesvåg, R., Jørgensen, K. N., Lange, E. H., Hartberg, C. B., Haukvik, U. K., … Agartz, I. (2016). Auditory Cortex Characteristics in Schizophrenia: Associations With Auditory Hallucinations. Schizophrenia Bulletin, **43**(1), 75–83.

Parga, A., Zafar, T., Nikulina, E.M. & Hammer, R.P. (2019) Excessive striatal dopamine activates auditory cortex via striato-pallido-thalamo-cortical circuits in the rat. Biological Psychiatry, submitted.

Patil, S. T., Zhang, L., Martenyi, F., Lowe, S. L., Jackson, K. A., Andreev, B. V., … Schoepp, D. D. (2007). *Activation of mGlu2/3 receptors as a new approach to treat schizophrenia: a randomized Phase 2 clinical trial. Nature Medicine, **13**(9), 1102–1107.*

Paxinos, G., Watson, C. (2007). The Rat Brain in Stereotaxic Coordinates. London: Academic Press.

Perez-Costas, E., Melendez-Ferro, M., & Roberts, R. C. (2010). Basal ganglia pathology in schizophrenia: dopamine connections and anomalies. Journal of Neurochemistry, **113**(2), 287–302.

"Predicted Irradiance Calculator." Predicted Irradiance Values: Model Based on Direct Measurements in Mammalian Brain Tissue, Optogenetic Resources at Stanford University, https://web.stanford.edu/group/dlab/cgi-bin/graph/chart.php.

Pycock CJ, Kerwin RW, Carter CJ (1980). Effect of lesion of cortical dopamine terminals on subcortical dopamine receptors in rats. Nature. 1980; **286**:74–76

Ring, H. A. (2002). *Neuropsychiatry of the basal ganglia. Journal of Neurology, Neurosurgery & Psychiatry, **72**(1), 12–21.*

Rolland, B., Jardri, R., Amad, A., Thomas, P., Cottencin, O., & Bordet, R. (2014). *Pharmacology of Hallucinations: Several Mechanisms for One Single Symptom? BioMed Research International, 2014, 1–9.*

Seeman, P. (2013). *Schizophrenia and dopamine receptors. European Neuropsychopharmacology, **23**(9), 999–1009.*

Seger, C. A. (2013). The visual corticostriatal loop through the tail of the caudate: circuitry and function. Frontiers in Systems Neuroscience, **7**.

Shergill, S. S., Brammer, M. J., Williams, S. C. R., Murray, R. M., & McGuire, P. K. (2000). Mapping Auditory Hallucinations in Schizophrenia Using Functional Magnetic Resonance Imaging. Archives of General Psychiatry, **57**(11), 1033.

Shin, S.E., Lee, J.S., Kang, M.H., Kim, C.E., Bae, J.N., Jung, G., 2005. Segmented volumes of cerebrum and cerebellum in first episode schizophrenia with auditory hallucinations. Psychiatry Research **138**, 33–42

Song, M., Yu, S. P., Mohamad, O., Cao, W., Wei, Z. Z., Gu, X., … Wei, L. (2017). Optogenetic stimulation of glutamatergic neuronal activity in the striatum enhances neurogenesis in the subventricular zone of normal and stroke mice. *Neurobiology of disease*, ***98***, 9–24

Veening, J. G., Cornelissen, F. M., & Lieven, P. A. J. M. (1980). *The topical organization of the afferents to the caudatoputamen of the rat. A horseradish peroxidase study. Neuroscience, **5**(7), 1253–1268.*

Vollenweider, F. X., & Geyer, M. A. (2001). *A systems model of altered consciousness: integrating natural and drug-induced psychoses. Brain Research Bulletin, **56**(5), 495–507.*

Wichmann, T., & Dostrovsky, J. O. (2011). Pathological basal ganglia activity in movement disorders. *Neuroscience*, ***198***, 232–244.

Zhuo, C., Zhu, J., Qin, W., Qu, H., Ma, X., & Yu, C. (2017). Cerebral blood flow alterations specific to auditory verbal hallucinations in schizophrenia. British Journal of Psychiatry, **210**(03), 209–215.